

Osteoblast mineralization requires beta1 integrin/ICAP-1-dependent fibronectin deposition.

Molly Brunner, Angélique Millon-Frémillon, Genevieve Chevalier, Inaam A. Nakchbandi, Deane Mosher, Marc R. Block, Corinne Albiges-Rizo, Daniel Dysad Erl 3148 Bouvard

▶ **To cite this version:**

Molly Brunner, Angélique Millon-Frémillon, Genevieve Chevalier, Inaam A. Nakchbandi, Deane Mosher, et al.. Osteoblast mineralization requires beta1 integrin/ICAP-1-dependent fibronectin deposition.. Journal of Cell Biology, 2011, 194 (2), pp.307-22. 10.1083/jcb.201007108 . inserm-00610020

HAL Id: inserm-00610020

https://inserm.hal.science/inserm-00610020

Submitted on 20 Jul 2011

HAL is a multi-disciplinary open access archive for the deposit and dissemination of scientific research documents, whether they are published or not. The documents may come from teaching and research institutions in France or abroad, or from public or private research centers.

L'archive ouverte pluridisciplinaire **HAL**, est destinée au dépôt et à la diffusion de documents scientifiques de niveau recherche, publiés ou non, émanant des établissements d'enseignement et de recherche français ou étrangers, des laboratoires publics ou privés.

Osteoblast mineralization requires β1 integrin/ICAP-1-dependent fibronectin deposition

Running title: ICAP-1 regulates osteoblast mineralization

eTOC Summary: *Icap-1* prevents recruitment of kindlin-2 to β1 integrin to control dynamics of fibrillar adhesion sites, fibronectin deposition, and osteoblast mineralization during bone formation.

Ms#201007108R2

Molly Brunner[1,2,3#], Angélique Millon-Frémillon[1,2,3#], Genevieve Chevalier[1,2,3], Inaam A. Nakchbandi[4], Deane Mosher[5], Marc Block[1,2,3], Corinne Albigès-Rizo[1,2,3§] and Daniel Bouvard[1,2,3§]

1: INSERM U823, Institut Albert Bonniot, Equipe1 DySAD, Grenoble, France
2: ERL CNRS 3148, Grenoble, France
3: Université Joseph Fourier, Grenoble, France
4: Max Planck Institute of Biochemistry and University of Heidelberg, Martinsried, Germany
5: School of Medicine and Public Health, University of Wisconsin, USA

§ to whom correspondence should be addressed:

Daniel Bouvard or Corinne Albigès-Rizo

INSERM U823, Institut Albert Bonniot, ERL CNRS 3148
Site Santé BP170 La Tronche
38042 Grenoble cedex 9
France
Tel: +33 476549552
Fax: +33 476549425
Email: daniel.bouvard@ujf-grenoble.fr, corinne.albiges-rizo@ujf-grenoble.fr

# Both authors equally contributed to the work

Characters counts: 40000

Key words : integrin, ICAP-1, osteogenesis, mineralization, kindlin

ABSTRACT

The morphogenetic and differentiation events required for bone formation are orchestrated by diffusible and insoluble factors that are localized within the extracellular matrix. In mice, the deletion of ICAP-1, a modulator of β1 integrin activation, leads to severe defects in osteoblast proliferation, differentiation, and mineralization and to a delay in bone formation. Deposition of fibronectin and maturation of fibrillar adhesions, adhesive structures that accompany fibronectin deposition, are impaired upon ICAP-1 loss, as are type I collagen deposition and mineralization. Expression of β1 integrin with a mutated binding site for ICAP-1 recapitulates the ICAP-null phenotype. Follow-up experiments demonstrated that ICAP-1 negatively regulates kindlin-2 recruitment onto the β1 integrin cytoplasmic domain whereas an excess of kindlin-2 binding has a deleterious effect on fibrillar adhesion formation. These results suggest that ICAP-1 works in concert with kindlin-2 to control the dynamics of β1 integrin-containing fibrillar adhesions and thereby regulates fibronectin deposition and osteoblast mineralization.

INTRODUCTION

The extracellular matrix controls tissue integrity, function, and differentiation (Rozario and Desimone, 2009). The proteins and proteoglycans in the extracellular matrix depend largely on the tissue (Manabe et al., 2008). Several matrix proteins such as fibronectin, laminins, or collagens mediate cell adhesion and support cell differentiation. In addition to the role of its various components in interacting with cells, the physical properties of the extracellular matrix are of paramount importance in defining cell fate and behavior. For instance, human mesenchymal stem cells (hMSC) cultured on matrix of various degrees of stiffness undergo different cell fates so that compliant matrix drives cells to become neuronal like while stiffer surfaces trigger differentiation of the hMSC into osteoblasts (Engler et al., 2006). Finally, the extracellular matrix acts as a reservoir for signaling molecules (Hynes, 2009); this function appears to be particularly important for bone tissue (Ramirez and Rifkin, 2009). Thus, signaling proteins such as the BMPs (bone morphogenetic proteins) or FGFs (fibroblast growth factors) are sequestered by the extracellular matrix in active conformations (Dallas et al., 2005; Fontana et al., 2005). Such sequestration appears to be crucial not only during development but also to coordinate bone resorption and deposition (Matsuo, 2009).

Integrins are the main class of receptors implicated in cell-extracellular matrix interactions (Hynes, 1992). These receptors trigger cell adhesion and transmit outside-in and inside-out signals and thereby are involved in numerous cellular functions such as proliferation, apoptosis, cell fate decision, and extracellular matrix organization (Giancotti and Ruoslahti, 1999). One of the most obvious functions of the extracellular matrix and of cell adhesion receptors is to control developmental processes. Indeed, the importance of various integrin family members for tissue-specific development or function has been unraveled by the use of

genetically modified mice in which specific integrins have been targeted (Bouvard et al., 2001).

Bones are formed by the close interplay between osteoblasts, which are bone matrix depositing cells, and osteoclasts, which are bone-resorbing cells. The precise function of the different integrins in bone homeostasis is rather puzzling, inasmuch as data reported on osteoblasts are contradictory. While some *in vitro* data strongly suggest that β1 integrins are critical for osteoblast differentiation and function, the role of β1 integrins *in vivo* is less clear (Hamidouche et al., 2009; Moursi et al., 1996; Wang et al., 2006; Xiao et al., 1998). Cell type-specific cre-mediated deletion of β1 integrin in the osteoblast lineage directed by the 2.3 kb type I collagen promoter leads to minor developmental and functional defects resulting from a defect in mechano-transduction in the osteocytes (Phillips et al., 2008). The minor phenotype suggests either an important compensatory effect from other integrins such as αv forming heterodimers with other β subunit or/and an early role of β1 integrins that was not revealed due to its late deletion. Similarly, the expression of a dominant negative form of β1 integrin in mature osteoblasts shows only mild effects on bone formation (Zimmerman et al., 2000).

The mild effects of targeting β1 integrin in late osteoblast lineage contrast with the phenotypic analysis of *Icap-1* (Itgb1bp1^{tm1Ref})-deficient mice. ICAP-1 is a small protein that interacts in a specific manner with the β1A integrin cytoplasmic domain (Chang et al., 1997; Zhang and Hemler, 1999). It negatively regulates talin binding onto β1 integrin and thereby would be expected to limit integrin activation (Bouvard et al., 2007; Bouvard et al., 2006; Bouvard et al., 2003; Millon-Fremillon et al., 2008). Germline deletion of *Icap-1* in mouse impairs osteoblast differentiation and proliferation *in vitro* and *in vivo*. *Icap-1*-deficient osteoblasts display defects of adhesion, compaction, and migration (Bouvard et al., 2007;

Millon-Fremillon et al., 2008), which explains at least partly the bone phenotype observed *in vivo*.

In this paper we provide a molecular explanation of how ICAP-1, likely by direct binding onto β1 integrin, affects osteoblast function. We show that fibronectin assembly is controlled by the binding of ICAP-1 to the β1 integrin tail and that such binding is required for bone mineralization. Our results reveal the critical role of ICAP-1 in modulating the dynamics of fibrillar adhesions, which are adhesive structures responsible for fibronectin deposition. We demonstrate that the control of matrix assembly by ICAP-1/ β1 integrin interaction plays an important role in governing essential developmental events such as osteoblast mineralization. We also provide evidence that ICAP-1 negatively regulates recruitment of kindlin-2 onto β1 integrin cytoplasmic domain and that an excess of kindlin-2 binding has a deleterious effect on fibrillar adhesion formation.

MATERIALS AND METHODS

Mice and Antibodies

Mice with a targeted mutation on *Icap-1* locus (Itgb1bp1^{tm1Ref}) were genotyped as previously reported (Bouvard et al., 2007). Mouse strains with floxed alleles of the genes encoding β1 integrin (Itgb1^{tm1Ref}) and fibronectin (Fn1^{tm1Ref}) have been described previously (Brakebusch et al., 2000; Potocnik et al., 2000; Sakai et al., 2001).

Polyclonal anti-ICAP-1 antibodies were described previously (1:1500; Bouvard and Block, 1998). Monoclonal antibodies against actin (A2066; 1:1000), vinculin (clone hVIN1; 1:2000), and talin (clone 8d4; 1:200), as well as the polyclonal antibodies against fibronectin (F3648, 1:1000) and kindlin-2 (K3269; 1:1000), were from Sigma-Aldrich (L'Isle d'Abeau, France). The polyclonal anti-β1 integrin serum was from Chemicon (Millipore, Molsheim, France; 1:1500). The polyclonal anti-β1 integrin cytoplasmic domain antibody was described previously (Martel et al., 2001). The monoclonal anti-β1 integrin antibodies 9EG7 and MB1.2 were from Becton Dickinson/Pharmingen (Le Pont de Claix, France; 1:100) and Millipore (Molsheim, France; 1:100), respectively. Anti-phosphotyrosine monoclonal antibody 4G10 used as hybridoma supernatant was produced in our laboratory. The monoclonal anti-eGFP antibody (b-2; 1:1000) was from Santa Cruz (USA).

Plasmids

β1-expressing construct was based on pCLMFG retroviral vector in which the wild-type human β1 integrin has been directionally inserted using EcoR1 and Not1 sites. D759A and V787T mutations were introduced in β1 integrin by Quickchange mutation kit Qiagen (Courtaboeuf, France) and verified by sequencing. Expression of mRFP-tensin was carried out using the pCLMFG-mRFP-tensin plasmid as described (Stanchi et al., 2009). Functional

upstream domain (FUD) arises from the first fibronectin binding motif of the *streptococcus pyogenes* adhesin protein F1. It encompasses the 43 residues of UD (upstream non repetitive domain) plus the first 6 residues of the first 37-residue repeat of the RD5 region (Tomasini-Johansson et al., 2001). FUD was produced recombinantly as described (Ensenberger et al., 2004). pCLMFG-eGFP-Kindlin2 was from Dr. R Fässler (MPI, Martinsried, Germany). cDNA encoding talin head domain was extracted from pBS/SK-/talin 1-1445 (gift from Dr. Hynes) using Spe1 and EcoRV sites and inserted in the pEGFP-N1 plasmid by SalI restriction after refilling.

Isolation, immortalization, infection and *In vitro* Cre mediated deletion of osteoblasts

A primary mouse osteoblast-enriched cell population was isolated from newborn calvaria by using a mixture of 0.3 mg/ml collagenase type I (Sigma-Aldrich) and 0.25% trypsin (Invitrogen/Gibco, Cergy-Pointoise, France) as described previously (Bellows et al., 1986; Bouvard et al., 2007). Cells were grown in α-MEM medium containing 10% FCS. Primary osteoblasts (passage 2) were immortalized by transduction with a retrovirus expressing the large SV40 T antigen (Fässler et al., 1995), cloned, and tested for their ability to induce alkaline phophatase (ALP) upon differentiation (Mansukhani et al., 2000), as previously described (Bouvard et al., 2007). At least 5 clones from wild-type or floxed mice were isolated. Rescue of ICAP-1 or β1 integrin expression in null cells was performed via retroviral infection using the pCLMFG-*Icap*-IRES-EGFP and the pCLMFG-β1 vectors, respectively, as previously described (Bouvard et al., 2007; Millon-Fremillon et al., 2008). β1 and fibronectin floxed immortalized osteoblasts were infected with an adenoviral supernatant encoding the Cre recombinase (kindly provided by Dr. R. Meuwissen, Institut Albert Bonniot, Grenoble France) for 1 hour in PBS supplemented with 2% FCS and 1 mM $MgCl_2$.

Solid phase assay and pull-down assay

ICAP-1 binding onto the cytoplasmic tail of $\beta1^{WT}$ or $\beta1^{V787T}$ integrin was carried out using an enzyme-linked immunosorbent assay. A 96-well tray (MaxiSorp, Nunc, Dutsher Brumath, France) was coated overnight at 4°C with various concentrations of His-ICAP-1 (0, 1, 5µg/ml) and blocked for 1 hour at room temperature with a 3% BSA/PBS solution. GST (5µg/well), BSA (3%) alone, or GST-tagged cyto-$\beta1^{WT}$ and cyto-$\beta1^{V787T}$ (10µg/well) were incubated for 1 hour at 37°C. After three washes with 3% BSA/ 0.01% Tween-20/ PBS, the cyto-$\beta1^{WT}$ and cyto-$\beta1^{V787T}$ peptides were detected using a polyclonal antibody against the β1 cytoplasmic tail for 45 min at 37°C and an HRP-conjugated secondary antibody (Biorad, Marnes la Coquette, France) for an additional 45 min at 37°C. Peroxidase activity was visualized using ABTS reagent at 405 nm. The efficiency of ICAP-1 binding onto cyto-$\beta1^{WT}$ or cyto-$\beta1^{V787T}$ was expressed after subtraction of GST and BSA signals.

Pull-down assays for talin and kindlin-2 were carried out as previously described (Lad et al., 2007). In brief, either HEK 293 or ICAP-1 transfected HEK 293 cells were washed with cold PBS and lysed by scraping in 0.5-ml cell lysis buffer (50 mM NaCl, 10 mM Pipes, 150 mM sucrose, 50 mM NaF, 40 mM Na4P2O7.10H2O, 1 mM Na3VO4, pH 6.8, 0.5% Triton X-100, 0.1% sodium deoxycholate, and EDTA-free protease inhibitor tablet) on ice. Cell lysate was cleared by centrifugation at 15000g for 30 min at 4°C. Lysate (500µg) was incubated with 10µg of GST-β1, GST-β3, or GST coated beads for 2 hours at 4°C. After three washes in lysis buffer, beads were resuspended in 2X Laemmli buffer, and samples were used in Western blotting to visualize talin and kindlin-2.

Compaction assay in hanging drops

Immortalized cells were harvested by trypsin digestion and washed twice in DMEM medium. Drops of 10 µl of DMEM-FCS (10%) medium containing 25,000 cells were spotted onto the

cover lid of 10 cm Petri dishes, inverted, and placed on a Petri dish containing 8 ml of PBS. Spheroid compaction was then followed over a 72-hour period, and images were taken with a binocular microscope equipped with a digital camera.

When ROCK inhibitor Y27632 (Calbiochem, France) was used, cells were resuspended into DMEM-FCS supplemented with 10 μM of Y27632 and then spotted on the cover-lid as described above.

Osteoblast differentiation

In vitro differentiation of isolated osteoblasts was performed essentially as previously described (Globus et al., 1998). In brief, 60,000 cells per well were plated in a 24-well tray. After 3 days of culture, when cells were confluent, the medium was switched to differentiation medium (α-MEM, 10% FCS, 50 μg/ml ascorbic acid, 10 mM β-glycerophosphate) and changed every other day. The differentiation process was visualized by alkaline phosphatase (ALP) staining for osteoblast activity and by Alizarin Red S staining for calcium deposition, as described (Bouvard et al., 2007). For collagen gel mineralization, highly concentrated type I collagen solution was used (9.3 mg/ml, Becton Dickinson/Pharmingen, Le Pont de Claix, France). A total of 300μl of type I collagen (5 mg/ml final concentration) containing $8x10^5$ cells per gel was loaded in a 24-well plate. Gels were grown for 1 week and then placed in differentiation medium for 3 weeks. Gels were stained directly with Alizarin RedS dye or cryo-sectioned before staining.

Visualization and quantification of fibronectin deposition and secretion

Cells (10^4) were seeded into a 24-well tray and cultured for 3 days in complete medium. Matrix-associated fibronectin was extracted after cell lysis in deoxycholate-containing buffer and centrifugation (15,000 rpm, 30 minutes, 4°C) as previously described (Schwarzbauer,

1991). The pellet fraction containing the pool of fibronectin associated within the matrix is referred to as “insoluble Fn”, whereas supernatant fibronectin is referred to as “soluble Fn”. Western blotting was done as described previously (Bouvard et al., 1998). Quantification of fibronectin in soluble and insoluble fractions was performed using Image J. Samples were also blotted for vinculin (1:1500) or actin (1:1500) to ensure that the same amounts of protein were loaded. ROCK inhibitor Y27632 (Merck Bioscience, Nottingham, UK) was used at the final concentration of 10 μM and added to cells seeded into a 24-well tray.

For fibronectin secretion, cells were incubated overnight in serum-free condition. Both culture supernatant and cells were used to visualize by Western blot the amount of secreted and cellular fibronectin. Band intensity was quantified using Image J software.

For cellular fibronectin, cells were resuspended in trypsin/EDTA. Trypsin was then blocked with Soybean trypsin inhibitor and cells were washed twice in PBS (this treatment leads to an undetectable amount of cell surface-associated fibronectin as measured by FACS). Then cells were lysed in RIPA buffer and equal amounts of protein were loaded on gel for Western blot in order to quantify fibronectin expression.

RNA isolation and real-time quantitative PCR

Total RNA was harvested from wild-type and *Icap-1*-null cell cultures by the NucleoSpin RNA II Kit (Macherey-Nagel) according to the manufacturer’s instructions. Then, 1.5μg of total RNA was reverse-transcribed using SuperScript VILO cDNA Synthesis Kit (Invitrogen) and 0.4μl of the resulting cDNA reaction mix was subjected to quantitative PCR using the GoTaq qPCR Master Mix (Promega) in a Stratagene Mx3005P Real-Time PCR System. Real time data were collected for 40 cycles at 95°C for 30 seconds, 55°C for 1 min, and 72°C for 30 seconds. Mouse primers for fibronectin and collagen I were respectively the following: 5-ATGTGGACCCCTCCTGATAGT-3 (forward) and 5-GCC CAG TGA TTT CAG CAA

AGG-3 (reverse), 5-CCT GGT AAA GAT GGG CC-3 (forward) and 5-CAC CAG GTT CAC CTT TCG CAC C-3 (reverse). The level of RNA for *Icap-1*-null cells compared to wild-type cells and normalized to Ranbp1 was calculated using the comparative Ct method of quantification.

Time-lapse video microscopy

mRFP-tensin-expressing osteoblasts were seeded in complete medium on uncoated Labtek chambers (NalgeNunc, Dutsher) and imaged as previously described (Millon-Fremillon et al., 2008). In brief, after overnight spreading, cells were subjected to time lapse videomicroscopy using an Axiovert200M microscope (Carl Zeiss, SAS, Le Pecq, France) equipped with a thermostatic chamber. Images were acquired every 5 minutes over a 6 hours period. Out of the stack, 3 images corresponding to 3 different time points were then selected and overlapped using Metamorph software after subtracting cell displacement. The centripetal translocation of fibrillar adhesions was shown by arbitrarily coloring each time-point image.

FACS, Immunohistology and immunofluorescence

FACS analysis and immunohistology were performed as described (Bouvard et al., 2007). For immunofluorescence, cells were fixed with 4% paraformaldehyde, permeabilized with 0.2% Triton X-100 (this step was omitted in the case of fibronectin staining), and incubated with appropriate primary antibodies. After being rinsed, coverslips were incubated with an appropriate AlexaFluor-conjugated secondary antibody. The cells were mounted in Mowiol/DAPI solution and imaged on an inverted confocal microscope (LSM510; Carl Zeiss).

RESULTS

Osteoblast cell compaction depends on fibronectin organization

We previously demonstrated that *in vitro* bone nodule formation is defective in the absence of the ICAP-1 protein (Bouvard et al., 2007). Because ICAP-1 interacts with β1 integrin (Bouvard et al., 2003; Chang et al., 1997; Zhang and Hemler, 1999) and despite the contradictory data concerning β1 integrins and bone formation described in the Introduction, we examined the roles of β1 integrins and a major ligand, fibronectin, in osteoblast function. Primary osteoblasts from $\beta1^{fl/fl}$ or $Fn^{fl/fl}$ mice were immortalized, and the gene of interest was deleted by viral transduction with Cre recombinase. Deletion was confirmed by immunostaining and FACS analysis for β1 integrin (Figure S1) and by Western blotting for fibronectin (Figure S2C). The resulting cell lines retained their ability to differentiate into osteoblasts, and the following results were confirmed for at least two separate lines of each (Bouvard et al., 2007; Chiba et al., 1993).

Inasmuch as osteoblast condensation occurs during early differentiation, we asked whether β1 integrins were required in this process (Hall and Miyake, 2000), especially since ICAP-1 loss leads to abnormal compaction at 24 hours (Fig. 1A and (Bouvard et al., 2007)). $\beta1^{-/-}$ cells were unable to form spheroids, in contrast to wild-type or rescue cells (Fig. 1B) and, instead, they formed only small aggregates, presumably due to the presence of cadherins that mediated cell-cell adhesions (Stains and Civitelli, 2005). Since α5β1 integrin has been shown to be critical for fibronectin deposition and organization (Hynes et al., 1992), we therefore examined whether the defect in osteoblast compaction could result from a defect in fibronectin deposition. For this purpose we analyzed osteoblasts lacking fibronectin. These fibronectin-null cells were unable to form spheroids, in contrast to the wild-type (Fig. 1C).

Thus, cell compaction requires both β1 integrins and their extracellular ligand fibronectin. Fibronectin might either activate specific signals or provide an extracellular scaffold that allows cell compaction. To distinguish these two possibilities, we used a 49-residue peptide called FUD that has been shown to bind to multiple N-terminal type I modules of fibronectin and thereby inhibit assembly of fibronectin into an insoluble matrix (Ensenberger et al., 2004; Ensenberger et al., 2001; Maurer et al., 2010; Tomasini-Johansson et al., 2001; Zhou et al., 2008). Treating the osteoblasts with FUD resulted in abnormal compaction, suggesting that fibronectin deposition is required for compaction to proceed normally (Fig. 1C). FUD treatment neither alters cell shape nor proliferation, and therefore adhesion mediated by β1 integrins was presumably not affected (Fig. S2). To confirm the key role of fibronectin fibrillogenesis in mediating β1 integrin effects on osteoblast compaction, we inhibited fibrillogenesis by using a ROCK inhibitor. RhoA/ROCK act downstream of α5β1 and mediate cell contractility required during compaction and for fibronectin fibrillogenesis (Yoneda et al., 2007; Zhong et al., 1998). Confirming previous data, the inhibition of ROCK reduced the insoluble fraction of fibronectin and hence the deposition of fibronectin in the extracellular matrix (Schwarzbauer, 1991; Zhong et al., 1998) (Fig. 1D). ROCK inhibition also reduced osteoblast compaction (Fig. 1D). It has been proposed that ICAP-1 might be involved in ROCK membrane targeting in myoblasts (Stroeken et al., 2006). We therefore wondered whether the effect of ICAP-1 on osteoblast compaction could be due to inefficient ROCK signaling. *Icap-1*-deficient cells were treated with the ROCK inhibitor Y27632, and both fibronectin deposition and cell compaction were analyzed. As shown in Fig. 1D, inhibition of ROCK in *Icap-1*-deficient cells further blocked fibronectin assembly relative to ROCK inhibition alone or to ICAP-1-deficient cells, which shows an additive effect. This finding suggests that ROCK and ICAP-1 do not belong to the same linear signaling pathway but rather to separate pathways. In summary, our data show that β1 integrin, ICAP-1, and

fibronectin are required for osteoblast compaction and suggest that β1 integrin effects on compaction are mediated by its ability to modulate fibronectin assembly.

Icap-1 loss reduces fibronectin deposition

The nodule formation assays for osteoblast function were performed in 3D cultures. To determine whether fibronectin defect could be extended to 2D cultures that would be suited for multi-probe fluorescence microscopy, the experiments were repeated using cells seeded on plates. We investigated whether matrix-associated fibronectin deposition could be perturbed by the loss of ICAP-1. Indeed, both wild-type and rescue cells displayed a larger fraction of matrix-associated insoluble fibronectin than *Icap-1*-null osteoblasts (Fig. 2A and 2B) (insoluble to soluble ratio in control cells: 1.3±0.2 vs. 0.7±0.2 in *Icap-1*-deficient cells, $p<0.001$). Immunolabeling of fibronectin on cultured cells showed that most of the cells in *Icap*-null cultures were associated with punctate deposits of fibronectin whereas most of the ICAP-1-expressing cells were associated with dense deposits of fibronectin (Fig. 2C). Similar results were obtained on spheroids cultures, showing that fibronectin fibrillogenesis defect was not restricted to 2D culture conditions (Fig S3 A-C). Importantly, there was no reduction in fibronectin expression and secretion in *Icap-1*-deficient cells as measured by quantitative PCR (qPCR) and Western blotting. Indeed, fibronectin mRNA expression and fibronectin secreted to medium were increased when ICAP-1 was lost (Fig. S3D). Thus, the defect in fibronectin assembly observed in *Icap-1*-null cells was not due to a decrease in fibronectin expression or secretion.

Direct β1 integrin/Icap-1 interaction controls fibronectin assembly by osteoblasts

We previously reported that ICAP-1 regulates β1 integrin function by reducing its affinity, likely by impairing talin recruitment (Bouvard et al., 2003; Millon-Fremillon et al., 2008). To determine whether ICAP-1-mediated down-regulation of β1 integrin affinity is involved in

fibronectin fibrillogenesis, we generated various point mutations in the human β1 integrin cytoplasmic domain that have been reported to interfere with specific functions. One of those is the mutation at valine 787, which is important for ICAP-1 binding on β1 integrin (Chang et al., 2002). To minimize a potential side effect of this mutation on the recruitment of other molecules such as kindlins, we generated a mutated β1 in which valine 787 was replaced by a threonine. This point mutation mimics the membrane-distal part of the β2 integrin cytoplasmic tail that does not bind ICAP-1 despite its high similarity with β1 integrin while still binding other proteins such as kindlins (Chang et al., 2002; Moser et al., 2009). The V787T mutation resulted in decreased ICAP-1 binding to β1 integrin without interfering with the binding of kindlin-2 and talin head (Fig. S4). The $\beta1^{V787T}$ integrin mutant was introduced into β1-null osteoblasts, and positive cells were selected by FACS based on human β1 expression (Fig. S1A). Compared to control cells, osteoblasts expressing the $\beta1^{V787T}$ integrin showed a significant decrease in insoluble matrix-bound fibronectin (Fig. 3A & 3B). In line with this observation, fibronectin immunofluorescent staining in confluent cultures of $\beta1^{V787T}$ cells revealed less fibronectin deposition than in control cells (Fig. 3C). Altogether, the defect in fibronectin fibrillogenesis observed in both *Icap-1*-null cells and $\beta1^{V787T}$ cells strongly suggests that efficient fibronectin fibrillogenesis requires the direct binding of ICAP-1 onto the β1 integrin cytoplasmic tail.

The introduction of D759A point mutation into β1 integrin (known to trigger a pre-activation state (Hughes et al., 1996; Sakai et al., 1998)) reproduced the effect of the lack of ICAP-1 on focal adhesion dynamics (Millon-Fremillon et al., 2008). We therefore asked whether this mutation also alters fibronectin fibrillogenesis. In line with previous results with fibroblasts (Sakai et al., 1998), $\beta1^{D759A}$ osteoblasts did not reduce fibronectin deposition significantly (Fig. 3). Next, we wondered whether the fibronectin fibrillogenesis defect observed in *Icap-1*-

null cells was associated with altered fibronectin reorganization. Wild-type, rescue, and *Icap-1*-null osteoblasts were seeded on a fibronectin coat, cultured for 3 hours, fixed, and double-stained for fibronectin and β1 integrin in order to visualize the capability of the cells to reorganize the surrounding extracellular matrix (Fig. 4). Whereas wild-type and rescue cells reorganized the fibronectin coating into fibrils that partially co-distributed with fibrillar arrays of β1 integrins, only minimal redistribution of fibronectin or fibrillar arrays of integrins were observed with *Icap-1*-null osteoblasts (Fig. 4A). Treatment of wild-type cells with the FUD peptide also blocked fibronectin redistribution in this assay (Fig. 4B). These findings suggest that ICAP-1 controls fibrillar adhesion dynamics, which in turn leads to fibronectin matrix reorganization.

Fibrillar adhesion dynamics are impaired in Icap-1-null cells

Based on the evidence that ICAP-1 is likely required for fibronectin fibrillogenesis via its direct binding onto β1 integrin and modulation of movement of β1 integrins into fibrillar adhesions, we further analyzed the molecular organization of adhesive structures. Thus, we immunostained cultured cells for fibronectin, talin, and β1 (Fig. 5). As shown in previous experiments, *Icap-1*-deficient osteoblasts exhibited reduced staining for fibronectin (Fig. 5A). Talin staining in wild-type and *Icap-1*-null cells was located at the periphery of both cells but in thinner and more elongated streaks in mutant cells than in control cells (Fig. 5B). Thus, in wild-type cells, talin appears to preferentially remain within focal adhesions rather than following fibrillar adhesions. When talin and β1 integrin were co-stained in wild-type cells, talin was concentrated at the cell periphery whereas β1 integrin displayed a different distribution pattern with extended streaks originating from the cell edge and pointing to the cell center. Co-staining of *Icap-1*-null cells demonstrated co-localization of talin and β1

integrin throughout the length of the streaks. Image analysis corroborated that talin and β1 integrin distribution patterns were different in *Icap-1*-null and wild-type cells (Fig. 5C). Thus, in *Icap-1*-deficient cells, talin and β1 integrin co-localized in adhesive structures, suggesting that β1 integrins are not translocated normally into fibrillar adhesions or fibrillar adhesion formation is somehow otherwise impaired.

To analyze fibrillar adhesion dynamics further, we generated *Icap-1*-deficient and wild-type cells expressing mRFP tagged tensin, a marker of fibrillar adhesions (Zamir et al., 1999). We took advantage of the dual localization of tensin to focal and fibrillar adhesions to follow its translocation from one structure to another. Both control and *Icap-1*-deficient cells were seeded on fibronectin-coated glass coverslips in the absence of serum, resulting in tensin localization at peripheral focal adhesions (Fig. 6A). After 1 hour of adhesion, the serum-free medium was replaced by serum containing complete medium to increase cell contractility and enable fibronectin fibrillogenesis (Zhang et al., 1994). After 4 hours, the cells were fixed, and mRFP fluorescence was analyzed to localize tensin. As shown in figure 6A, at time 0 tensin was concentrated at the cell periphery in all genotypes. After addition of complete medium to wild-type and rescue cells, tensin moved centrally, conversely to *Icap-1*-null cells in which tensin remained at the cell edges (Fig. 6A). The apparent perturbation of tensin dynamics upon ICAP-1 loss was confirmed using time-lapse video microscopy of wild-type and *Icap-1*-null cells expressing mRFP-tensin that were seeded on glass coverslips in complete medium (Fig. 6B). As expected, in wild-type cells, time course analysis of mRFP-tensin localization showed translocation from the cell edge to cell center (Zamir et al., 1999). In contrast, in *Icap-1*-null osteoblasts, tensin translocation was not directionally oriented towards the cell center, but rather the protein kept a static localization (Fig. 6B). This defect in fibrillar adhesion formation was further confirmed using a β1 integrin antibody in the pulse chase experiment (Pankov et al., 2000) (Fig. S5). While control cells displayed clear β1 integrin

translocation from peripheral focal adhesions sites to fibrillar adhesions, *Icap-1*-deficient cells displayed only faint β1 staining close to the cell edge, suggesting a profound perturbation of β1 dynamics. These results all indicate that ICAP-1 has an important role in the dynamics of fibrillar adhesions and provide a reasonable explanation for the fibronectin deposition defect observed in *Icap-1*-deficient cells.

Icap-1 regulates recruitment of kindlin-2 on β1 integrin cytoplasmic domain

ICAP-1 and kindlins interact with an overlapping binding site on the cytoplasmic domain of β1 integrin (Chang et al., 1997; Larjava et al., 2008; Ma et al., 2008; Meves et al., 2009; Montanez et al., 2008; Zhang and Hemler, 1999). Therefore, we addressed the potential effect of ICAP-1 in the regulation of kindlin-2 binding on β1 integrin. First, we made use of *Icap-1*-deficient cells and $\beta1^{V787T}$ integrin mutant to analyze whether loss of ICAP-1 binding on β1 integrin could affect kindlin-2 localization. $\beta1^{fl/fl}$, *Icap-1*$^{-/-}$, and $\beta1^{V787T}$ were transduced with eGFP-Kindlin-2 retrovirus to generate cell lines. Based on eGFP expression, clones were selected for their expression level (Fig S4, and data not shown). Interestingly, high expression of eGFP-kindlin-2 was achieved readily in control cells but always low in *Icap*-1-deficient cells as well as in $\beta1^{V787T}$ mutant cells, already suggesting a molecular interaction. Kindlin-2 localization in focal adhesions was easily detectable in $\beta1^{V787T}$ and *Icap-1*-deficient cells, while control cells displayed faint staining, mainly at the cell edge (Fig. 7A). Increasing the expression of kindlin-2 in control cells was associated with a greater localization at focal adhesion sites (data not shown). This observation suggested that ICAP-1 negatively regulates kindlin-2 localization within focal adhesions. To address the role of ICAP-1 in regulating kindlin-2 binding on β1 integrin cytoplasmic domain more directly, we expressed ICAP-1 in HEK 293 cells and analyzed whether ICAP-1 modulates the interaction of kindlin-2 with GST-β1 fusion protein in a pull-down assay. ICAP-1 over-expression significantly reduced

the amount of kindlin-2 in GST-β1 pull-down assays, again arguing that ICAP-1 negatively regulates kindlin-2 binding on β1 integrin (Fig. 7B).

To explore whether part of the *Icap-1*-null phenotype is due to an excess of kindlin-2 binding onto β1 integrin, we selected an osteoblast cell line in which kindlin-2 expression was maximal (Fig S4) and used it to see whether fibronectin fibrillogenesis proceeded correctly. Such overexpression of kindlin-2 dramatically reduced fibronectin deposition, relative to non-transfected cells (Fig. 7C).

Matrix-associated fibronectin controls osteoblast mineralization

We previously reported that *Icap-1*-null mice exhibit decreased osteoblast proliferation, differentiation, and mineralization, resulting in a distinct bone phenotype (Bouvard et al., 2007). On the other hand, fibronectin has been shown to be crucial for osteoblast differentiation and survival *in vitro* and *in vivo* (Bentmann et al., 2009; Moursi et al., 1996; Moursi et al., 1997). We therefore examined whether the mineralization defect of *Icap-1*-null osteoblasts might be due to the defect in fibronectin fibrillogenesis described above. For this, we monitored the *in vitro* mineralization capabilities of osteoblasts expressing $\beta1^{fl/fl}$ (wild-type), $\beta1^{-/-}$, $\beta1^{WT}$ (rescue), $\beta1^{D759A}$, and $\beta1^{V787T}$. As expected, the induction of differentiation of wild-type and rescue β1 osteoblasts resulted in the appearance of mineralized bone nodules, revealed by Alizarin Red S staining at day 20 (ARS) (arrows in Fig. 8). We also observed mineralization with the $\beta1^{D759A}$ mutant (arrows in Fig. 8), which agrees with the fact that this point mutation does not impair fibronectin deposition (Fig. 3). Although the color uptake varied depending on the speed of mineralization, we constantly observed bone nodules when osteoblasts expressing $\beta1^{fl/fl}$ (rescue), $\beta1^{WT}$, and $\beta1^{D759A}$ were used, in sharp contrast to osteoblasts expressing $\beta1^{-/-}$ and $\beta1^{V787T}$, which were unable to form mineralized bone nodules despite their ability to express alkaline phosphatase, an early marker of osteoblast

commitment (Fig. 8). Interestingly, osteoblasts expressing $\beta1^{-/-}$ and $\beta1^{V787T}$ also displayed a fibronectin deposition defect, similar to that of *Icap-1*-null osteoblasts (Fig. 2 & 3). These observations suggest that fibronectin organization is crucial for osteoblast mineralization. To test by a second approach whether fibronectin organization is required for proper mineralization, we blocked fibronectin assembly in wild-type cells by FUD and followed mineralization. In contrast to untreated wild-type cells, which displayed extensive mineralization, FUD-treated cells showed a significant reduction in mineralization (Fig. 9A). Again, as we observed for cells with altered β1 integrin, the expression of alkaline phosphatase was still detectable, showing that treated cells have retained their capacity to commit to osteoblasts. Together, these data indicate that fibronectin organization is crucial for osteoblast mineralization.

We next considered how fibronectin influences mineralization and hypothesized that fibronectin directs deposition of other molecules to support mineralization. Since fibronectin directly binds to type I collagen and is important for its deposition, we immunostained for type I collagen control (wild-type), *Icap-1*$^{-/-}$, or $\beta1^{-/-}$ osteoblasts during their differentiation (Fig. 9B). In contrast to controls that clearly showed a significant and reproducible increase in collagen immunoreactivity after differentiation, *Icap-1*- as well as β1-deficient cells did not increase their amount of type I collagen. Very similar results were obtained when control cells were treated with FUD (data not shown). These results show that fibronectin is an important regulator of type I collagen deposition by osteoblasts. To relate the lack of mineralization in cultures of mutant cells with the absence of "mineralizable" matrix, we seeded control, and *Icap-1*- and β1-deficient cells in gels containing a high concentration of collagen. Induction of differentiation led to mineralization in both control and *Icap-1*-deficient osteoblasts although to a much lower extent in *Icap-1*-null osteoblasts (Fig. 9C). β1-integrin-deficient osteoblasts also displayed mineralization but to a much lower extent than control cells, likely reflecting

their profound defect in proliferation (Fig. 9C). Therefore, by providing an appropriate matrix, *Icap-1*$^{-/-}$ cells were able to mineralize, demonstrating that *in vitro* the absence of mineralization is primarily due to an altered matrix.

Since the effect of a lack of ICAP-1 on fibronectin deposition could be reproduced by kindlin-2 overexpression, we asked whether this phenocopy could be extended to the mineralization defect. Indeed, overexpression of kindlin-2 strongly repressed mineralization, supporting our previous findings (Fig. 9D). Altogether, these data highlight a novel important function of ICAP-1 in regulating kindlin-2 recruitment on β1 integrin and the subsequent extracellular matrix organization.

DISCUSSION

Icap-1 regulates fibronectin assembly in a β1-integrin-dependent manner

The experiments described herein define a new role for ICAP-1 in facilitating fibronectin fibrillogenesis. Our investigations explain why germline deletion of *Icap-1* in mouse impairs osteoblast differentiation and proliferation *in vitro* and *in vivo*, and why *Icap-1*-deficient osteoblasts display defects of adhesion, compaction, and migration.

Building on our previous studies demonstrating increased assembly of focal adhesions in the absence of ICAP-1 (Millon-Fremillon et al., 2008), we show here that loss of ICAP-1 perturbs the maturation of focal adhesions into fibrillar adhesions. Interestingly, expressing pre-activated integrin bearing mutation D759A reproduced the altered dynamics of focal adhesions seen in *Icap-1*-null cells but not the reduced fibronectin fibrillogenesis. Reconciling this apparent discrepancy calls for more extensive work, but it is likely that the transition of focal adhesions to fibrillar adhesions requires cycling and/or recruitment of critical proteins. Supporting this view is the distribution of talin, which is more concentrated in focal adhesions than in fibrillar adhesions. Conversely, tensin is almost absent from focal adhesions (for cells cultured in complete medium) but enriched in fibrillar adhesions. Thus one can easily envision that focal and fibrillar adhesion dynamics, formation, or initiation might be differentially regulated. In such a model, the importance of the salt bridge of the α and β1 integrin cytoplasmic tails might be more important in one context than the other. Talin, which has been reported to disrupt the salt bridge (Anthis et al., 2009), is more concentrated in focal adhesion. The salt bridge disruption may be less important for the dynamics of fibrillar adhesions, which contain little talin, and be instead controlled by other tail-effector interactions. In any case, our findings are consistent with the absence of obvious phenotype in a knock-in mouse model expressing the D759A mutation (Czuchra et al., 2006).

The effect of ICAP-1 on the cell ability to assemble fibronectin fibers was likely dependent on the direct interaction between ICAP-1 and the β1 integrin chain, as ascertained by the finding that expression of mutated β1 integrin with reduced ICAP-1 affinity recapitulates both defects: i.e., the lack of fibronectin assembly and mineralization defect. Furthermore, we provide evidence that ICAP-1 plays an important role in regulating the recruitment of β1 integrins to fibrillar adhesions and thereby the dynamics of fibrillar adhesions.

These results support the view that fibrillar adhesions and focal adhesions are distinct structures with specific composition and dynamics (Cukierman et al., 2001; Green et al., 2009). In addition, the two adhesion types support different functions of β1 integrins: focal adhesions for cell adhesion, and fibrillar adhesions for deposition and organization of the extracellular matrix. How these structures are related is an open question. Locking integrin affinity would be expected to cause defects in spreading and migration mediated by focal adhesions or in extracellular matrix organization mediated by fibrillar adhesions. One interesting observation is the segregation of β1 integrins in either focal adhesions or fibrillar adhesions depending on the cellular context. We always observed formation of fibrillar adhesion sites when cells were cultured on uncoated substrate. Conversely, forcing β1 integrin into focal adhesions by seeding cells on concentrated fibronectin-coated surfaces or blocking fibronectin assembly was associated with reduced fibrillar adhesions but increased focal adhesion formation. Our hypothesis is that either ICAP-1 loss or increase in kindlin-2 expression favors β1 localization at focal adhesion sites and disfavors its recruitment at fibrillar adhesions. However, this view does not rule out that β1 integrin could be required at an early stage in focal adhesion assembly before being engaged in fibrillar adhesions. This would explain why cells need β1 integrin activation for fibrillar adhesions to be formed (Green et al., 2009). Loss of ICAP-1 would interfere with the release of integrin-associated

proteins such as kindlin and talin in focal adhesions and thereby would reduce the formation or maturation of fibrillar adhesion sites. Additional work should be done to decipher at the molecular level how β1 integrin participates in focal to fibrillar adhesion assembly. But for the first time, our present work points out the importance of integrin cellular adaptors in this process.

ILK, PINCH, parvins, and kindlins belong to a protein complex that is involved in fibrillar adhesion maturation (Stanchi et al., 2009; Vouret-Craviari et al., 2004). Loss of kindlins in mice leads to severe phenotypes associated with integrin dysfunction in cells (Moser et al., 2009; Moser et al., 2008; Ussar et al., 2008). Kindlins bind to the most distal NPxY motif on the β1 integrin cytoplasmic tail (Meves et al., 2009), where the ICAP-1 binding site has also been mapped (Chang et al., 1997). Thus, the two proteins would be expected to compete for the same overlapping site. This hypothesis is supported by our experiments demonstrating that the loss of ICAP-1 or the expression of a β1 integrin mutation within the ICAP-1 binding site increase kindlin-2 recruitment on the β1 integrin cytoplasmic domain and within focal adhesion sites. ILK, which is recruited at focal adhesion via kindlin-2 in worm and C2C12 cells (Dowling et al., 2008; Mackinnon et al., 2002), is also involved in fibronectin deposition (Stanchi et al., 2009). Although the interplay among ILK, ICAP-1, and kindlin-2 remains to be unraveled, one may now place ILK downstream of ICAP-1 as well as kindlin-2.

Fibronectin fibrillogenesis is required for osteoblast mineralization

Both the composition and the physical state of the extracellular matrix play an important role in controlling osteoblast differentiation and mineralization. For instance, hMSC cultured on stiff matrix preferentially commit to the osteoblast lineage (Engler et al., 2006; McBeath et al., 2004). The extracellular matrix can affect osteoblast differentiation both by providing specific integrin binding sites and by acting as a reservoir for small signaling molecules such

as BMPs or FGFs (Grunert et al., 2007; Margosio et al., 2003). Several reports have established the involvement of the extracellular matrix in osteoblast differentiation and mineralization (Moursi et al., 1996; Moursi et al., 1997). Indeed, fibronectin has been shown important for osteoblast differentiation and survival (Moursi et al., 1996; Moursi et al., 1997). Our present study not only provides important molecular mechanisms explaining these data, but also shows the first direct experimental evidence that fibronectin assembly in itself is crucial for mineralization. By modulating β1 integrin translocation into fibrillar adhesions, ICAP-1 regulates the amount, the structure, and the assembly of matrix-associated fibronectin, which is important for the formation of a competent extracellular matrix allowing proper mineralization. Our attempts to identify the specific integrin receptors involved in this process by using blocking antibodies raised against specific α subunits have failed, possibly due to quick endocytosis of the antibodies during the course of the experiment (unpublished data). However, considering the predominant role of the α5β1 integrin for fibronectin fibrillogenesis, it is likely that this integrin is also crucial for mineralization. It has been reported that fibronectin serves as scaffolding matrix for additional extracellular proteins such as collagens and TGF-β, but also for sequestering and presenting diffusible factors such as BMPs and FGFs (Huang et al., 2009; Hynes, 2009; Sottile and Hocking, 2002). Therefore, interfering with fibronectin assembly will affect the overall matrix environment, making it less permissive for proper mineralization. In line with our present data is the observation that the maintenance of an extracellular matrix of fibronectin as well as collagen requires continuous fibronectin assembly (Shi et al., 2010; Sottile and Hocking, 2002).

Fibronectin is important for osteoblast compaction

Osteoblast compaction is an important early step during their differentiation (Lecanda et al., 2000). In the absence of efficient fibronectin assembly, osteoblast compaction was severely

reduced. Therefore, *Icap-1*-deficient osteoblasts that displayed reduced fibronectin deposition were unable to properly compact. Similarly, osteoblasts deficient in β1 integrin expression had a severe defect in cell compaction. Consistent with our findings, fibronectin is important for cell compaction of mesenchymal cells, showing that a proper extracellular matrix also supports cell compaction in the mesenchymal cell lineage (Robinson et al., 2004; Salmenpera et al., 2008). Surprisingly, cadherins expressed on osteoblasts (Stains and Civitelli, 2005) are not sufficient to support efficient cell compaction in the absence of β1 integrin even though small cell aggregates were observed in β1-null osteoblasts, suggesting that cadherins could be involved at earlier stages. More investigations will be necessary to address the exact function of cadherins during this process.

ROCK has been shown to interact with ICAP-1 (Stroeken et al. 2006). In our present work, we did not evidence any linear connection between ICAP-1 and ROCK in the regulation of cell compaction. Indeed, inhibition of ROCK as well as loss of ICAP-1 expression led to cell compaction and fibronectin deposition defect. However, ROCK inhibition in *Icap-1*-deficient cells further reduced cell compaction and fibronectin fibrillogenesis, suggesting that both proteins may act through distinct signaling pathways. Such ROCK-dependent pathways could be activated via the fibronectin receptor syndecan, as recently proposed (Wang et al., 2010).

In conclusion we report a molecular mechanism for the osteoblast differentiation defect that is present in *Icap-1*-deficient mice. ICAP-1, likely by interacting directly with β1 integrin, is important for translocation of β1 integrins into fibrillar adhesions, which are required for proper fibronectin self-assembly into fibrils. Moreover we show that fibronectin assembly in turn allows mineralization. Thus for the first time, we provide the mechanism by which ICAP-1 affects bone mineralization at a late stage of osteoblast differentiation.

Acknowledgments

We are grateful to Pr. Reinhard Fässler for providing us with β1 integrin and Fn floxed mice, EGFP-Kindlin2 construct and for critical reading of the manuscript. We also thank Drs. Martin Humphries and M. Billaud for their critical reading and suggestions. We thank Dr Alexei Grichine for microscopy and Dr Juliana Ribeyron, and Dr Sandrine De Seranno for FACS-sorting. M. Brunner is supported by a MRT fellowship and A. Millon-Fremillon by ARC. This research was supported by a Pro-A INSERM grant and Ligue contre le cancer (to D. Bouvard), NIH HL21644 (to D Mosher), Max-Planck Society and University of Heidelberg (to I. Nakchbandi) as well as ARC and Région Rhône-Alpes (to C. Albiges-Rizo). This work is dedicated to Rachel.

Legends to figure

Figure 1. *Cell matrix interaction and contractility are required for osteoblast compaction*

A. Cellular compaction of *Icap-1*$^{+/+}$ (wild-type), *Icap-1*^{WT} (rescue), and *Icap-1*$^{-/-}$ osteoblasts after 24 or 48 hours. Scale bar : 1 mm.

B. Cellular compaction of $\beta1^{fl/fl}$ (wild-type), $\beta1^{WT}$ (rescue), and $\beta1^{-/-}$ osteoblasts after 24 hours. Scale bar : 1 mm.

C. Cellular compaction after 24 hours of $Fn^{-/-}$ osteoblasts and $Fn^{fl/fl}$ (wild-type) treated or not with 100 ng/ml of FUD. Scale bar : 1 mm.

D. ROCK and ICAP-1 additive control of cell compaction and fibronectin deposition. Upper panel: Fibronectin deposition was monitored in *Icap-1*$^{+/+}$ (wild-type) and *Icap-1*$^{-/-}$ osteoblasts treated with DMSO (control) or ROCK inhibitor (Y27632). Fibronectin amounts (Fn) were estimated by Western blotting, and protein load was normalized using actin (Act) (left). Quantification of fibronectin deposition from 3 independent experiments using Image J software (right). Lower panel: Cell compaction of *Icap-1*$^{+/+}$ (wild-type) and *Icap-1*$^{-/-}$ in presence of DMSO (control) or ROCK inhibitor (Y27632) were imaged after 24 hours. Scale bar : 1 mm.

Figure 2. *Icap-1*$^{-/-}$*osteoblasts in 2D culture exhibit a defect in fibronectin deposition*

A. *Icap-1*$^{+/+}$ (wild-type), *Icap-1*^{WT} (rescue), and *Icap-1*$^{-/-}$ cells were cultured for 3 days and then lysed in a buffer containing deoxycholate to separate the insoluble matrix-bound fibronectin (Ins) from the soluble fibronectin (Sol). Fibronectin amounts were estimated by Western blotting, and the protein load was normalized using actin.

B. Quantification of 10 independent experiments using Image J software. Quantifications are shown as the means and SD of the ratio of insoluble/soluble fibronectin fraction (* and **: significant difference with a p value of 0.001 and 0.0004 respectively; NS: no significant difference with a p value of 0.3).

C. Fibronectin deposition of *Icap-1*$^{-/-}$, *Icap-1*^{WT} (rescue), and *Icap-1*$^{+/+}$ (wild-type) cells in 2D culture. Cells were fixed and immunostained for fibronectin (red) and counterstained with DAPI (blue). Scale bar : 20 µm.

Figure 3. *Fibronectin fibrillogenesis requires β1 integrin in an ICAP-1 dependent manner*

A. $\beta1^{fl/fl}$ (wild-type), $\beta1^{WT}$ (rescue), $\beta1^{D759A}$, $\beta1^{-/-}$, and $\beta1^{V787T}$ cells were cultured for 3 days and then lysed in a buffer containing deoxycholate to separate the insoluble matrix-bound fibronectin (Ins) from the soluble fibronectin (Sol). Fibronectin amounts were estimated by Western blotting and the protein load was normalized using actin.

B. Quantification of four independent experiments using Image J software. Quantifications are shown as ratio of insoluble/soluble fibronectin fraction (** and *: significant difference with a p value of 0.001 and 0.015 respectively; NS: no significant difference with a p value of 0.18).

C. $\beta1^{WT}$ (rescue), $\beta1^{fl/fl}$ (wild-type), $\beta1^{D759A}$, $\beta1^{-/-}$, and $\beta1^{V787T}$ cells were fixed and immunostained for fibronectin and counterstained with DAPI. Scale bar : 10 µm.

Figure 4. *Fibronectin reorganization depends on Icap-1 and its ability to self-assemble*

A. *Icap-1*$^{+/+}$ (wild-type), *Icap-1*^{WT} (rescue), and *Icap-1*$^{-/-}$ cells were seeded on fibronectin-coated coverslips. After 4 hours of incubation, cells were fixed and immunostained for β1 integrin (green) and for total fibronectin (red). Scale bar : 10 µm.

B. Wild-type cells were seeded on fibronectin in the presence of FUD (*Icap-1*$^{+/+}$ +FUD) or not. After 4 hours of incubation, cells were fixed and immunostained for β1 integrin (green) and for total fibronectin (red). Scale bar : 10 µm.

Figure 5. *Fibrillar adhesion formation is defective in Icap-1*$^{-/-}$ *osteoblasts*

A. *Icap-1*$^{+/+}$ (wild-type) or *Icap-1*$^{-/-}$ osteoblasts were seeded on fibronectin-coated coverslips in complete medium. After overnight incubation, the cells were fixed and immunostained for talin (red) and fibronectin (green) and counterstained with DAPI (blue). Scale bar : 10 µm.

B. Immunostaining of talin (red) and β1 integrin (green) counterstained with DAPI (blue) of *Icap-1*$^{+/+}$ (wild-type) or *Icap-1*$^{-/-}$ osteoblasts. Scale bar : 10 µm. A typical area used for pixel plot analysis is boxed.

C. Pixel intensity profile along focal adhesion for talin (red) and β1 integrin (green) is represented from cell edge to cell center. These plots are representative of at least ten different plots analyzed.

Figure 6. *Tensin dynamics are impaired in Icap-1*$^{-/-}$ *osteoblasts*

A. Localization of mRFP-tensin in *Icap-1*$^{+/+}$ (wild-type), *Icap-1*^{WT} (rescue), and *Icap-1*$^{-/-}$ cells in the absence (T = 0H) or presence (T = 4H) of serum. Arrows indicate peripheral focal adhesions; arrow heads indicate dorsal fibrillar adhesions. Scale bar : 10 µm.

B. Time-lapse video microscopy of mRFP-tensin in *Icap-1*$^{+/+}$ (wild-type) and *Icap-1*$^{-/-}$ osteoblasts seeded on glass coverslips. Frames at time 0, 30 minutes, and 300 minutes were extracted from a representative video and arbitrarily colored in green (time 0), red (time 30 minutes), and blue (time 300 minutes). Scale bar : 10 µm.

Figure 7. *ICAP-1 regulates fibrillogenesis by negatively regulating kindlin-2 binding on β1 integrin.*

A. eGFP-kindlin-2 localization in wild-type, $\beta1^{V787T}$, or *Icap-1*$^{-/-}$ cells seeded overnight on glass coverslips.

B. Kindlin-2 binding on β1 integrin in presence of a normal (mock) or high level of ICAP-1 (Icap-1) was analyzed using pull-down assays. Kindlin-2 binding on GST alone, GST-β1, and GST-β3 as well as ICAP-1 expression was visualized by Western blotting, and kindlin-2 bindings to GST-β1 (blue) and GST-β3 (green) were quantified from 3 independent experiments using Image J software (*: significant difference with a p value of 0.05).

C. Visualization of fibronectin deposition in cells expressing different levels of eGFP-kindlin-2 (from non-transfected cells (mock), moderate (medium), and high level (high)). Fibronectin deposition was visualized by immunofluorescence (upper panel) or after biochemical fractionation to determine the relative quantity of matrix-bound fibronectin (ins) and the non organized counterparts (sol) (lower panel). Data are representatives of 3 different experiments performed with 2 different clones (*: significant difference with a p value of 0.0009).

Figure 8. *β1 integrin regulates in vitro mineralization in an Icap-1-dependent manner*

$\beta1^{fl/fl}$ (wild-type), $\beta1^{WT}$ (rescue), $\beta1^{D759A}$, $\beta1^{V787T}$, and $\beta1^{-/-}$ cells were induced to differentiate into osteoblasts. Expression of alkaline phosphatase (ALP) was used to follow the early commitment of cells to the osteoblast lineage at day 0 (D0) and day 15 (D15). Mineralization was visualized by Alizarin RedS staining (ARS) at day 20 (D20). Arrows indicate mineralized bone nodules. Scale bar : 1 mm.

Figure 9. *Blocking fibronectin fibrillogenesis impairs mineralization*

A. Wild-type cells were induced to differentiate into osteoblasts in the presence (FUD treated) or absence (control) of FUD, and the expressions of alkaline phosphatase (ALP) and mineralization (ARS) were monitored at day 0 (D0) and day 14 (D14). Scale bar : 1 mm.

B. Wild-type ($\beta1^{fl/fl}$), *Icap-1*$^{-/-}$, and $\beta1^{-/-}$ cells were cultured as described for *in vitro* mineralization assay. At D0, medium was changed to induce differentiation. Cells were fixed either at D0 or D4, and type I collagen deposition was analyzed by immunofluorescence staining. Scale bar : 20 μm.

C. Wild-type ($\beta1^{fl/fl}$), *Icap-1*$^{-/-}$, and $\beta1^{-/-}$ cells were embedded in highly concentrated type I collagen gel (5 mg/ml). After 1 week in normal medium to allow cell proliferation, medium was changed for the osteogenic medium and culture continued for 21 additional days. Gels were then stained with Alizarin RedS to detect mineralized foci. Scale bar : 1 mm.

D. Mineralization of cells expressing high levels of kindlin-2 (high) was analyzed after their culture in osteoblast differentiation media. Expression of alkaline phosphatase (ALP) was used to follow the early commitment of cells to the osteoblast lineage at day 0 (D0) and mineralization was visualized by Alizarin RedS staining (ARS) at day 15 (D15). Scale bar : 1 mm.

Legends to supplementary figures

Figure S1. *Expression of β1 integrin and its mutated forms in β1-null osteoblasts.*

A. Wild-type ($\beta1^{fl/fl}$), β1-null ($\beta1^{-/-}$), and β1-null osteoblasts rescued with mutant β1 integrins ($\beta1^{V787T}$ and $\beta1^{D759A}$) were stained at 4°C with anti-mouse β1 integrin (mβ1, green) alone (top) or in combination with anti-human β1 integrin (hβ1, red) or anti-phosphotyrosine (PY, green).

Scale bar : 10 μm. In this and the second panel, cells with mutated β1 are denoted by the site of mutation.

B. FACS analysis of integrin surface expression using either anti-mouse β1 integrin (mβ1, red) or anti-human β1 integrin (hβ1; red: $\beta1^{-/-}$, green: $\beta1^{759}$, blue: $\beta1^{759}$) to detect ectopic expression of integrins.

Figure S2. *FUD treatment alters neither cell shape nor cell proliferation and survival*

A. After 4 hours of culture in complete medium in the presence of FUD (+FUD) or not (-FUD), wild-type osteoblasts were fixed and immunostained for β1 integrin and phosphotyrosine (PY) and counterstained with DAPI. Scale bar : 10 μm.

B. To analyze cell proliferation and survival, wild-type osteoblasts were counted after 48 or 72 hours of culture in the presence of FUD (+FUD) or not (-FUD).

C. Wild-type ($Fn^{fl/fl}$) and fibronectin-null ($Fn^{-/-}$) osteoblasts were cultured in complete medium and then lysed. Fibronectin amounts were estimated by Western blot analysis. Protein load was normalized using actin.

Figure S3. *Icap-1$^{-/-}$ spheroids exhibit a defect in fibronectin deposition that is not due to a defect in fibronectin and type I collagen expression or fibronectin secretion*

A. Spheroids formed from *Icap-1$^{+/+}$* (wild-type), *Icap-1^{WT}* (rescue), and *Icap-1$^{-/-}$* cells were fixed after 48 hours and frozen sections were immunostained for fibronectin and counterstained with DAPI. Scale bar : 20 μm.

B. *Icap-1$^{+/+}$* (wild-type), *Icap-1^{WT}* (rescue), and *Icap-1$^{-/-}$* spheroids were lysed in a buffer containing deoxycholate, followed by centrifugation to separate insoluble matrix-bound fibronectin (Ins) from soluble fibronectin (Sol). Fibronectin amounts were estimated by Western blot analysis.

C. Summary of results of four independent experiments for determining the ratio of soluble and insoluble fibronectin. Quantification was accomplished using Image J analysis software and is presented as the means and standard deviation (SD) of the ratio of insoluble/soluble fibronectin fraction (**: significant difference with a p value of <0.001; *: significant difference with a p value of <0.01).

D. Fibronectin expression and secretion in the supernatant of wild-type (*Icap-1*$^{+/+}$) and *Icap-1*-null (*Icap-1*$^{-/-}$) cell cultures were visualized by Western blot analyses and quantified using Image J software (upper panel, quantification of 5 independent experiments). Fibronectin and type I collagen mRNA levels were quantified using quantitative rtPCR (lower panel).

Figure S4. *β1*^{V787T} *integrin mutation interferes with ICAP-1 binding but not with kindlin-2 recruitment.*

A. ICAP-1 binding was assessed using solid phase assay and background on BSA and GST was subtracted. Specificity was also verified by absence of binding of his-ICAP-1 onto GST-cyto-β3 domain (unpublished).

B. Kindlin-2 and eGFP-Talin Head binding on wild-type or mutant (β1^{V787T}) β1 integrin was analyzed using pull-down assay. Bindings on GST alone, GST-β1, and GST-β1^{V787T} were visualized by Western blot. In this panel, cells with mutated β1 are denoted by the site of mutation.

C. Localization of eGFP-Kindlin-2 in β1^{V787T}-expressing cells. Cells were stably transduced with a supernatant containing retroviruses encoding eGFP-Kindlin-2. Cells were plated on fibronectin-coated glass coverslips, and localization of β1 integrin (red) was determined using 9EG7 antibody. Scale bar : 10 μm.

D. Wild-type (wt) cells expressing medium and high levels of eGFP-Kindlin-2 (medium and high respectively), *Icap-1*-null and cells expressing the mutated β1^{V787T} integrin were cultured in complete medium and then lysed. Kindlin-2 amounts were estimated by Western blot

analysis. The ratio of eGFP-Kindlin-2 fusion expression to endogenous kindlin-2 expression is indicated.

Figure S5. *Defect in the translocation of β1-containing fibrillar adhesion.*
Icap-1$^{+/+}$ and *Icap-1*$^{-/-}$ cells were seeded on fibronectin-coated glass coverslips for 4 hours. Live cells were incubated with 9EG7 anti-β1 integrin antibody for 30 minutes at 4°C, and then cells were either directly fixed (T = 0) or incubated at 37°C for an additional hour (T = 60). β1 integrin localization (red) was visualized by indirect immunofluorescence, phosphotyrosine (green) labeling was used to visualize focal adhesion, and nuclei were stained using DAPI (blue). Scale bar : 10 μm.

REFERENCES

Anthis, N.J., K.L. Wegener, F. Ye, C. Kim, B.T. Goult, E.D. Lowe, I. Vakonakis, N. Bate, D.R. Critchley, M.H. Ginsberg, and I.D. Campbell. 2009. The structure of an integrin/talin complex reveals the basis of inside-out signal transduction. *EMBO J*. 28:3623-32.

Bellows, C.G., J. Sodek, K.L. Yao, and J.E. Aubin. 1986. Phenotypic differences in subclones and long-term cultures of clonally derived rat bone cell lines. *J Cell Biochem*. 31:153-69.

Bentmann, A., N. Kawelke, D. Moss, H. Zentgraf, Y. Bala, I. Berger, J.A. Gasser, and I.A. Nakchbandi. 2009. Circulating Fibronectin Affects Bone Matrix While Osteoblast Fibronectin Modulates Osteoblast Function. *J Bone Miner Res*.

Bouvard, D., A. Aszodi, G. Kostka, M.R. Block, C. Albiges-Rizo, and R. Fässler. 2007. Defective osteoblast function in ICAP-1-deficient mice. *Development*. 134:2615-25.

Bouvard, D., C. Brakebusch, E. Gustafsson, A. Aszodi, T. Bengtsson, A. Berna, and R. Fässler. 2001. Functional consequences of integrin gene mutations in mice. *Circ Res*. 89:211-23.

Bouvard, D., A. Millon-Fremillon, S. Dupe-Manet, M.R. Block, and C. Albiges-Rizo. 2006. Unraveling ICAP-1 function: toward a new direction? *Eur J Cell Biol*. 85:275-82.

Bouvard, D., A. Molla, and M.R. Block. 1998. Calcium/calmodulin-dependent protein kinase II controls alpha5beta1 integrin-mediated inside-out signaling. *J Cell Sci*. 111 (Pt 5):657-65.

Bouvard, D., L. Vignoud, S. Dupe-Manet, N. Abed, H.N. Fournier, C. Vincent-Monegat, S.F. Retta, R. Fässler, and M.R. Block. 2003. Disruption of focal adhesions by integrin cytoplasmic domain-associated protein-1 alpha. *J Biol Chem*. 278:6567-74.

Brakebusch, C., R. Grose, F. Quondamatteo, A. Ramirez, J.L. Jorcano, A. Pirro, M. Svensson, R. Herken, T. Sasaki, R. Timpl, S. Werner, and R. Fässler. 2000. Skin and hair follicle integrity is crucially dependent on beta 1 integrin expression on keratinocytes. *EMBO J*. 19:3990-4003.

Chang, D.D., B.Q. Hoang, J. Liu, and T.A. Springer. 2002. Molecular basis for interaction between Icap1 alpha PTB domain and beta 1 integrin. *J Biol Chem*. 277:8140-5.

Chang, D.D., C. Wong, H. Smith, and J. Liu. 1997. ICAP-1, a novel beta1 integrin cytoplasmic domain-associated protein, binds to a conserved and functionally important NPXY sequence motif of beta1 integrin. *J Cell Biol*. 138:1149-57.

Chiba, H., N. Sawada, T. Ono, S. Ishii, and M. Mori. 1993. Establishment and characterization of a simian virus 40-immortalized osteoblastic cell line from normal human bone. *Jpn J Cancer Res*. 84:290-7.

Cukierman, E., R. Pankov, D.R. Stevens, and K.M. Yamada. 2001. Taking cell-matrix adhesions to the third dimension. *Science*. 294:1708-12.

Czuchra, A., H. Meyer, K.R. Legate, C. Brakebusch, and R. Fässler. 2006. Genetic analysis of beta1 integrin "activation motifs" in mice. *J Cell Biol*. 174:889-99.

Dallas, S.L., P. Sivakumar, C.J. Jones, Q. Chen, D.M. Peters, D.F. Mosher, M.J. Humphries, and C.M. Kielty. 2005. Fibronectin regulates latent transforming growth factor-beta (TGF beta) by controlling matrix assembly of latent TGF beta-binding protein-1. *J Biol Chem*. 280:18871-80.

Dowling, J.J., A.P. Vreede, S. Kim, J. Golden, and E.L. Feldman. 2008. Kindlin-2 is required for myocyte elongation and is essential for myogenesis. *BMC Cell Biol*. 9:36.

Engler, A.J., S. Sen, H.L. Sweeney, and D.E. Discher. 2006. Matrix elasticity directs stem cell lineage specification. *Cell*. 126:677-89.

Ensenberger, M.G., D.S. Annis, and D.F. Mosher. 2004. Actions of the functional upstream domain of protein F1 of Streptococcus pyogenes on the conformation of fibronectin. *Biophys Chem*. 112:201-7.

Ensenberger, M.G., B.R. Tomasini-Johansson, J. Sottile, V. Ozeri, E. Hanski, and D.F. Mosher. 2001. Specific interactions between F1 adhesin of Streptococcus pyogenes and N-terminal modules of fibronectin. *J Biol Chem*. 276:35606-13.

Fässler, R., M. Pfaff, J. Murphy, A.A. Noegel, S. Johansson, R. Timpl, and R. Albrecht. 1995. Lack of beta 1 integrin gene in embryonic stem cells affects morphology, adhesion, and migration but not integration into the inner cell mass of blastocysts. *J Cell Biol*. 128:979-88.

Fontana, L., Y. Chen, P. Prijatelj, T. Sakai, R. Fässler, L.Y. Sakai, and D.B. Rifkin. 2005. Fibronectin is required for integrin alphavbeta6-mediated activation of latent TGF-beta complexes containing LTBP-1. *FASEB J*. 19:1798-808.

Giancotti, F.G., and E. Ruoslahti. 1999. Integrin signaling. *Science*. 285:1028-32.

Globus, R.K., S.B. Doty, J.C. Lull, E. Holmuhamedov, M.J. Humphries, and C.H. Damsky. 1998. Fibronectin is a survival factor for differentiated osteoblasts. *J Cell Sci*. 111 (Pt 10):1385-93.

Green, J.A., A.L. Berrier, R. Pankov, and K.M. Yamada. 2009. beta1 integrin cytoplasmic domain residues selectively modulate fibronectin matrix assembly and cell spreading through talin and Akt-1. *J Biol Chem*. 284:8148-59.

Grunert, M., C. Dombrowski, M. Sadasivam, K. Manton, S.M. Cool, and V. Nurcombe. 2007. Isolation of a native osteoblast matrix with a specific affinity for BMP2. *J Mol Histol*. 38:393-404.

Hall, B.K., and T. Miyake. 2000. All for one and one for all: condensations and the initiation of skeletal development. *Bioessays*. 22:138-47.

Hamidouche, Z., O. Fromigue, J. Ringe, T. Haupl, P. Vaudin, J.C. Pages, S. Srouji, E. Livne, and P.J. Marie. 2009. Priming integrin alpha5 promotes human mesenchymal stromal cell osteoblast differentiation and osteogenesis. *Proc Natl Acad Sci U S A*. 106:18587-91.

Huang, G., Y. Zhang, B. Kim, G. Ge, D.S. Annis, D.F. Mosher, and D.S. Greenspan. 2009. Fibronectin binds and enhances the activity of bone morphogenetic protein 1. *J Biol Chem*. 284:25879-88.

Hughes, P.E., F. Diaz-Gonzalez, L. Leong, C. Wu, J.A. McDonald, S.J. Shattil, and M.H. Ginsberg. 1996. Breaking the integrin hinge. A defined structural constraint regulates integrin signaling. *J Biol Chem*. 271:6571-4.

Hynes, R.O. 1992. Integrins: versatility, modulation, and signaling in cell adhesion. *Cell*. 69:11-25.

Hynes, R.O. 2009. The extracellular matrix: not just pretty fibrils. *Science*. 326:1216-9.

Hynes, R.O., E.L. George, E.N. Georges, J.L. Guan, H. Rayburn, and J.T. Yang. 1992. Toward a genetic analysis of cell-matrix adhesion. *Cold Spring Harb Symp Quant Biol*. 57:249-58.

Lad, Y., D.S. Harburger, and D.A. Calderwood. 2007. Integrin cytoskeletal interactions. *Methods Enzymol*. 426:69-84.

Larjava, H., E.F. Plow, and C. Wu. 2008. Kindlins: essential regulators of integrin signalling and cell-matrix adhesion. *EMBO Rep*. 9:1203-8.

Lecanda, F., P.M. Warlow, S. Sheikh, F. Furlan, T.H. Steinberg, and R. Civitelli. 2000. Connexin43 deficiency causes delayed ossification, craniofacial abnormalities, and osteoblast dysfunction. *J Cell Biol*. 151:931-44.

Ma, Y.Q., J. Qin, C. Wu, and E.F. Plow. 2008. Kindlin-2 (Mig-2): a co-activator of beta3 integrins. *J Cell Biol*. 181:439-46.

Mackinnon, A.C., H. Qadota, K.R. Norman, D.G. Moerman, and B.D. Williams. 2002. C. elegans PAT-4/ILK functions as an adaptor protein within integrin adhesion complexes. *Curr Biol*. 12:787-97.

Manabe, R., K. Tsutsui, T. Yamada, M. Kimura, I. Nakano, C. Shimono, N. Sanzen, Y. Furutani, T. Fukuda, Y. Oguri, K. Shimamoto, D. Kiyozumi, Y. Sato, Y. Sado, H. Senoo, S. Yamashina, S. Fukuda, J. Kawai, N. Sugiura, K. Kimata, Y. Hayashizaki, and K. Sekiguchi. 2008. Transcriptome-based systematic identification of extracellular matrix proteins. *Proc Natl Acad Sci U S A*. 105:12849-54.

Mansukhani, A., P. Bellosta, M. Sahni, and C. Basilico. 2000. Signaling by fibroblast growth factors (FGF) and fibroblast growth factor receptor 2 (FGFR2)-activating mutations blocks mineralization and induces apoptosis in osteoblasts. *J Cell Biol*. 149:1297-308.

Margosio, B., D. Marchetti, V. Vergani, R. Giavazzi, M. Rusnati, M. Presta, and G. Taraboletti. 2003. Thrombospondin 1 as a scavenger for matrix-associated fibroblast growth factor 2. *Blood*. 102:4399-406.

Martel, V., C. Racaud-Sultan, S. Dupe, C. Marie, F. Paulhe, A. Galmiche, M.R. Block, and C. Albiges-Rizo. 2001. Conformation, localization, and integrin binding of talin depend on its interaction with phosphoinositides. *J Biol Chem*. 276:21217-27.

Matsuo, K. 2009. Cross-talk among bone cells. *Curr Opin Nephrol Hypertens*. 18:292-7.

Maurer, L.M., B.R. Tomasini-Johansson, W. Ma, D.S. Annis, N.L. Eickstaedt, M.G. Ensenberger, K.A. Satyshur, and D.F. Mosher. 2010. Extended binding site on fibronectin for the functional upstream domain (FUD) of protein F1 of Streptococcus pyogenes. *J Biol Chem*. 285:41087-99.

McBeath, R., D.M. Pirone, C.M. Nelson, K. Bhadriraju, and C.S. Chen. 2004. Cell shape, cytoskeletal tension, and RhoA regulate stem cell lineage commitment. *Dev Cell*. 6:483-95.

Meves, A., C. Stremmel, K. Gottschalk, and R. Fässler. 2009. The Kindlin protein family: new members to the club of focal adhesion proteins. *Trends Cell Biol*. 19:504-13.

Millon-Fremillon, A., D. Bouvard, A. Grichine, S. Manet-Dupe, M.R. Block, and C. Albiges-Rizo. 2008. Cell adaptive response to extracellular matrix density is controlled by ICAP-1-dependent beta1-integrin affinity. *J Cell Biol*. 180:427-41.

Montanez, E., S. Ussar, M. Schifferer, M. Bosl, R. Zent, M. Moser, and R. Fässler. 2008. Kindlin-2 controls bidirectional signaling of integrins. *Genes Dev*. 22:1325-30.

Moser, M., M. Bauer, S. Schmid, R. Ruppert, S. Schmidt, M. Sixt, H.V. Wang, M. Sperandio, and R. Fässler. 2009. Kindlin-3 is required for beta2 integrin-mediated leukocyte adhesion to endothelial cells. *Nat Med*. 15:300-5.

Moser, M., B. Nieswandt, S. Ussar, M. Pozgajova, and R. Fässler. 2008. Kindlin-3 is essential for integrin activation and platelet aggregation. *Nat Med*. 14:325-30.

Moursi, A.M., C.H. Damsky, J. Lull, D. Zimmerman, S.B. Doty, S. Aota, and R.K. Globus. 1996. Fibronectin regulates calvarial osteoblast differentiation. *J Cell Sci*. 109 (Pt 6):1369-80.

Moursi, A.M., R.K. Globus, and C.H. Damsky. 1997. Interactions between integrin receptors and fibronectin are required for calvarial osteoblast differentiation in vitro. *J Cell Sci*. 110 (Pt 18):2187-96.

Pankov, R., E. Cukierman, B.Z. Katz, K. Matsumoto, D.C. Lin, S. Lin, C. Hahn, and K.M. Yamada. 2000. Integrin dynamics and matrix assembly: tensin-dependent translocation of alpha(5)beta(1) integrins promotes early fibronectin fibrillogenesis. *J Cell Biol*. 148:1075-90.

Phillips, J.A., E.A. Almeida, E.L. Hill, J.I. Aguirre, M.F. Rivera, I. Nachbandi, T.J. Wronski, M.C. van der Meulen, and R.K. Globus. 2008. Role for beta1 integrins in cortical osteocytes during acute musculoskeletal disuse. *Matrix Biol*. 27:609-18.

Potocnik, A.J., C. Brakebusch, and R. Fässler. 2000. Fetal and adult hematopoietic stem cells require beta1 integrin function for colonizing fetal liver, spleen, and bone marrow. *Immunity*. 12:653-63.

Ramirez, F., and D.B. Rifkin. 2009. Extracellular microfibrils: contextual platforms for TGFbeta and BMP signaling. *Curr Opin Cell Biol*. 21:616-22.

Robinson, E.E., R.A. Foty, and S.A. Corbett. 2004. Fibronectin matrix assembly regulates alpha5beta1-mediated cell cohesion. *Mol Biol Cell*. 15:973-81.

Rozario, T., and D.W. Desimone. 2009. The extracellular matrix in development and morphogenesis: A dynamic view. *Dev Biol*.

Sakai, T., K.J. Johnson, M. Murozono, K. Sakai, M.A. Magnuson, T. Wieloch, T. Cronberg, A. Isshiki, H.P. Erickson, and R. Fässler. 2001. Plasma fibronectin supports neuronal survival and reduces brain injury following transient focal cerebral ischemia but is not essential for skin-wound healing and hemostasis. *Nat Med*. 7:324-30.

Sakai, T., Q. Zhang, R. Fässler, and D.F. Mosher. 1998. Modulation of beta1A integrin functions by tyrosine residues in the beta1 cytoplasmic domain. *J Cell Biol*. 141:527-38.

Salmenpera, P., E. Kankuri, J. Bizik, V. Siren, I. Virtanen, S. Takahashi, M. Leiss, R. Fässler, and A. Vaheri. 2008. Formation and activation of fibroblast spheroids depend on fibronectin-integrin interaction. *Exp Cell Res*. 314:3444-52.

Schwarzbauer, J.E. 1991. Identification of the fibronectin sequences required for assembly of a fibrillar matrix. *J Cell Biol*. 113:1463-73.

Shi, F., J. Harman, K. Fujiwara, and J. Sottile. 2010. Collagen I matrix turnover is regulated by fibronectin polymerization. *Am J Physiol Cell Physiol*. 298:in press.

Sottile, J., and D.C. Hocking. 2002. Fibronectin polymerization regulates the composition and stability of extracellular matrix fibrils and cell-matrix adhesions. *Mol Biol Cell*. 13:3546-59.

Stains, J.P., and R. Civitelli. 2005. Cell-cell interactions in regulating osteogenesis and osteoblast function. *Birth Defects Res C Embryo Today*. 75:72-80.

Stanchi, F., C. Grashoff, C.F. Nguemeni Yonga, D. Grall, R. Fässler, and E. Van Obberghen-Schilling. 2009. Molecular dissection of the ILK-PINCH-parvin triad reveals a fundamental role for the ILK kinase domain in the late stages of focal-adhesion maturation. *J Cell Sci*. 122:1800-11.

Stroeken, P.J., B. Alvarez, J. Van Rheenen, Y.M. Wijnands, D. Geerts, K. Jalink, and E. Roos. 2006. Integrin cytoplasmic domain-associated protein-1 (ICAP-1) interacts with the ROCK-I kinase at the plasma membrane. *J Cell Physiol*. 208:620-8.

Tomasini-Johansson, B.R., N.R. Kaufman, M.G. Ensenberger, V. Ozeri, E. Hanski, and D.F. Mosher. 2001. A 49-residue peptide from adhesin F1 of Streptococcus pyogenes inhibits fibronectin matrix assembly. *J Biol Chem*. 276:23430-9.

Ussar, S., M. Moser, M. Widmaier, E. Rognoni, C. Harrer, O. Genzel-Boroviczeny, and R. Fässler. 2008. Loss of Kindlin-1 causes skin atrophy and lethal neonatal intestinal epithelial dysfunction. *PLoS Genet*. 4:e1000289.

Vouret-Craviari, V., E. Boulter, D. Grall, C. Matthews, and E. Van Obberghen-Schilling. 2004. ILK is required for the assembly of matrix-forming adhesions and capillary morphogenesis in endothelial cells. *J Cell Sci*. 117:4559-69.

Wang, L., G. Zhao, R. Olivares-Navarrete, B.F. Bell, M. Wieland, D.L. Cochran, Z. Schwartz, and B.D. Boyan. 2006. Integrin beta1 silencing in osteoblasts alters substrate-dependent responses to 1,25-dihydroxy vitamin D3. *Biomaterials*. 27:3716-25.

Xiao, G., D. Wang, M.D. Benson, G. Karsenty, and R.T. Franceschi. 1998. Role of the alpha2-integrin in osteoblast-specific gene expression and activation of the Osf2 transcription factor. *J Biol Chem*. 273:32988-94.

Yoneda, A., D. Ushakov, H.A. Multhaupt, and J.R. Couchman. 2007. Fibronectin matrix assembly requires distinct contributions from Rho kinases I and -II. *Mol Biol Cell*. 18:66-75.

Zamir, E., B.Z. Katz, S. Aota, K.M. Yamada, B. Geiger, and Z. Kam. 1999. Molecular diversity of cell-matrix adhesions. *J Cell Sci*. 112 (Pt 11):1655-69.

Zhang, Q., W.J. Checovich, D.M. Peters, R.M. Albrecht, and D.F. Mosher. 1994. Modulation of cell surface fibronectin assembly sites by lysophosphatidic acid. *J Cell Biol*. 127:1447-59.

Zhang, X.A., and M.E. Hemler. 1999. Interaction of the integrin beta1 cytoplasmic domain with ICAP-1 protein. *J Biol Chem*. 274:11-9.

Zhong, C., M. Chrzanowska-Wodnicka, J. Brown, A. Shaub, A.M. Belkin, and K. Burridge. 1998. Rho-mediated contractility exposes a cryptic site in fibronectin and induces fibronectin matrix assembly. *J Cell Biol*. 141:539-51.

Zhou, X., R.G. Rowe, N. Hiraoka, J.P. George, D. Wirtz, D.F. Mosher, I. Virtanen, M.A. Chernousov, and S.J. Weiss. 2008. Fibronectin fibrillogenesis regulates three-dimensional neovessel formation. *Genes Dev*. 22:1231-43.

Zimmerman, D., F. Jin, P. Leboy, S. Hardy, and C. Damsky. 2000. Impaired bone formation in transgenic mice resulting from altered integrin function in osteoblasts. *Dev Biol*. 220:2-15.

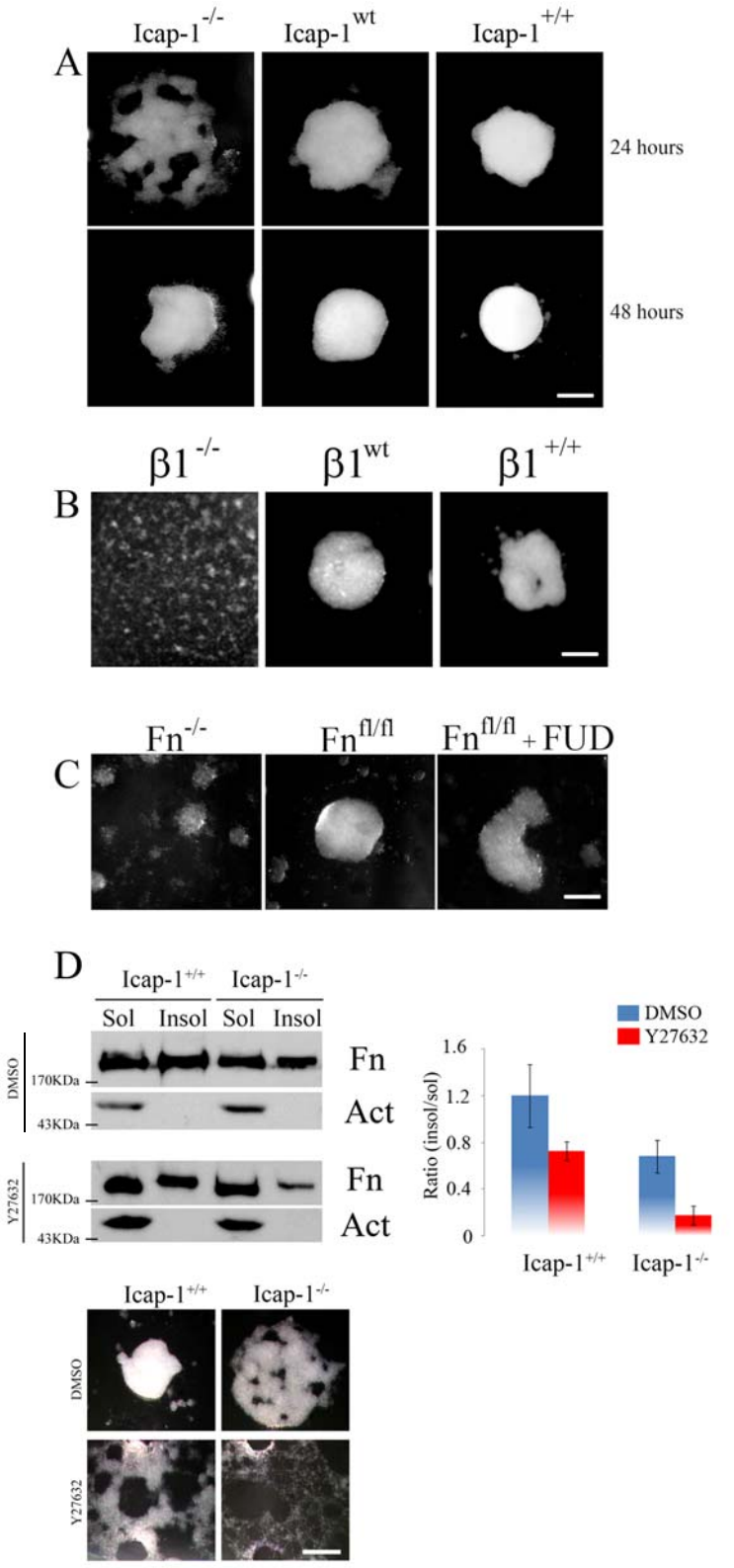

A
Icap-1 -/-
Icap-1 wt
Icap-1 +/+
24 hours
48 hours
B
β1 -/-
β1 wt
β1 +/+
C
Fn -/-
Fn fl/fl
Fn fl/fl + FUD
D
Icap-1 +/+
Icap-1 -/-
Sol
Insol
Sol
Insol
DMSO
170KDa
43KDa
Fn
Act
Y27632
170KDa
43KDa
Fn
Act
DMSO
Y27632
Ratio (insol/sol)
1.6
1.2
0.8
0.4
0
Icap-1 +/+
Icap-1 -/-
Icap-1 +/+
Icap-1 -/-
DMSO
Y27632

Fig. 1

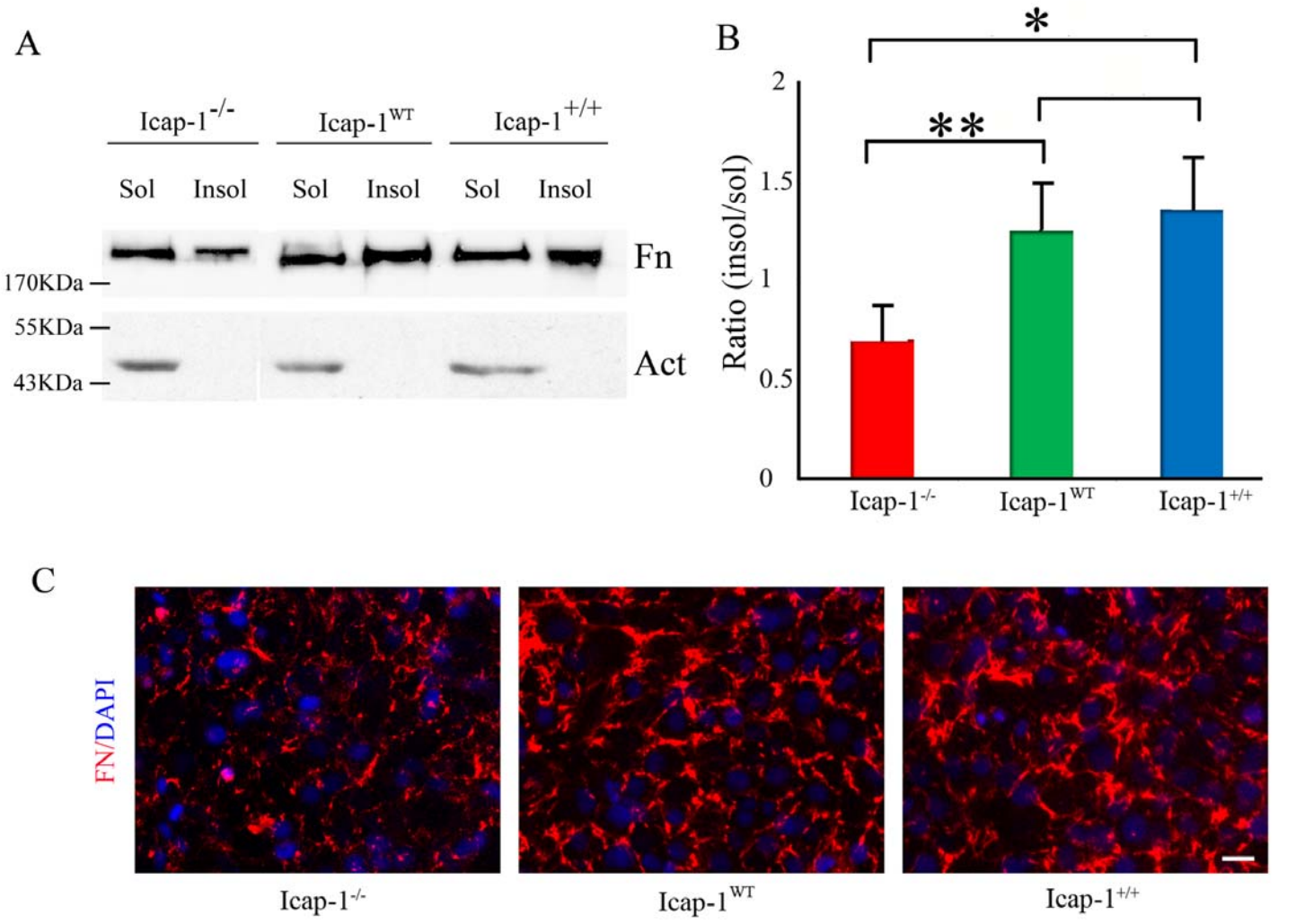

A
Icap-1-/-
Icap-1WT
Icap-1+/+
Sol
Insol
Sol
Insol
Sol
Insol
Fn
Act
170KDa
55KDa
43KDa
B
*
**
Ratio (insol/sol)
2
1.5
1
0.5
0
Icap-1-/-
Icap-1WT
Icap-1+/+
C
FN/DAPI
Icap-1-/-
Icap-1WT
Icap-1+/+

Fig. 2

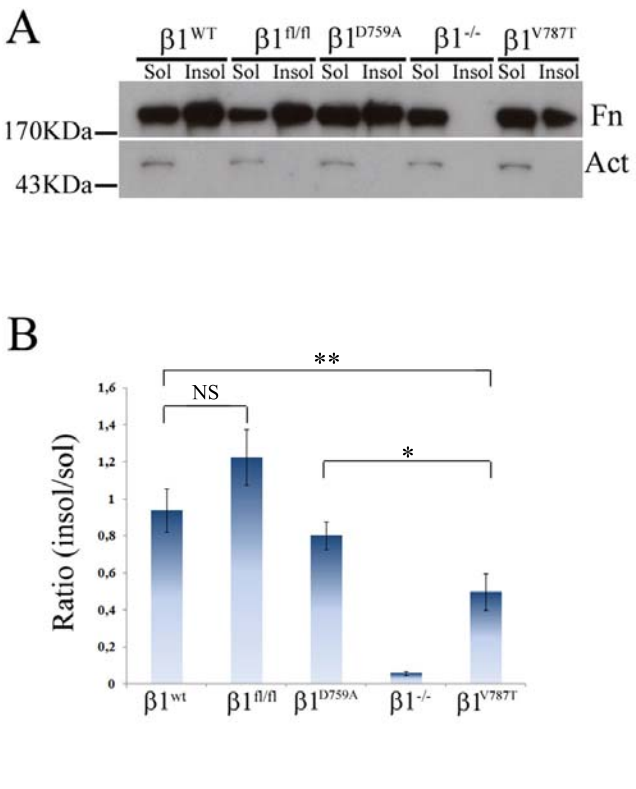

A
β1WT
β1fl/fl
β1D759A
β1-/-
β1V787T
Sol Insol Sol Insol Sol Insol Sol Insol Sol Insol
170KDa
43KDa
Fn
Act
B
Ratio (insol/sol)
NS
**
*
β1wt
β1fl/fl
β1D759A
β1-/-
β1V787T
C
β1fl/fl
β1V787T
β1wt
β1D759A
β1-/-

Fig. 3

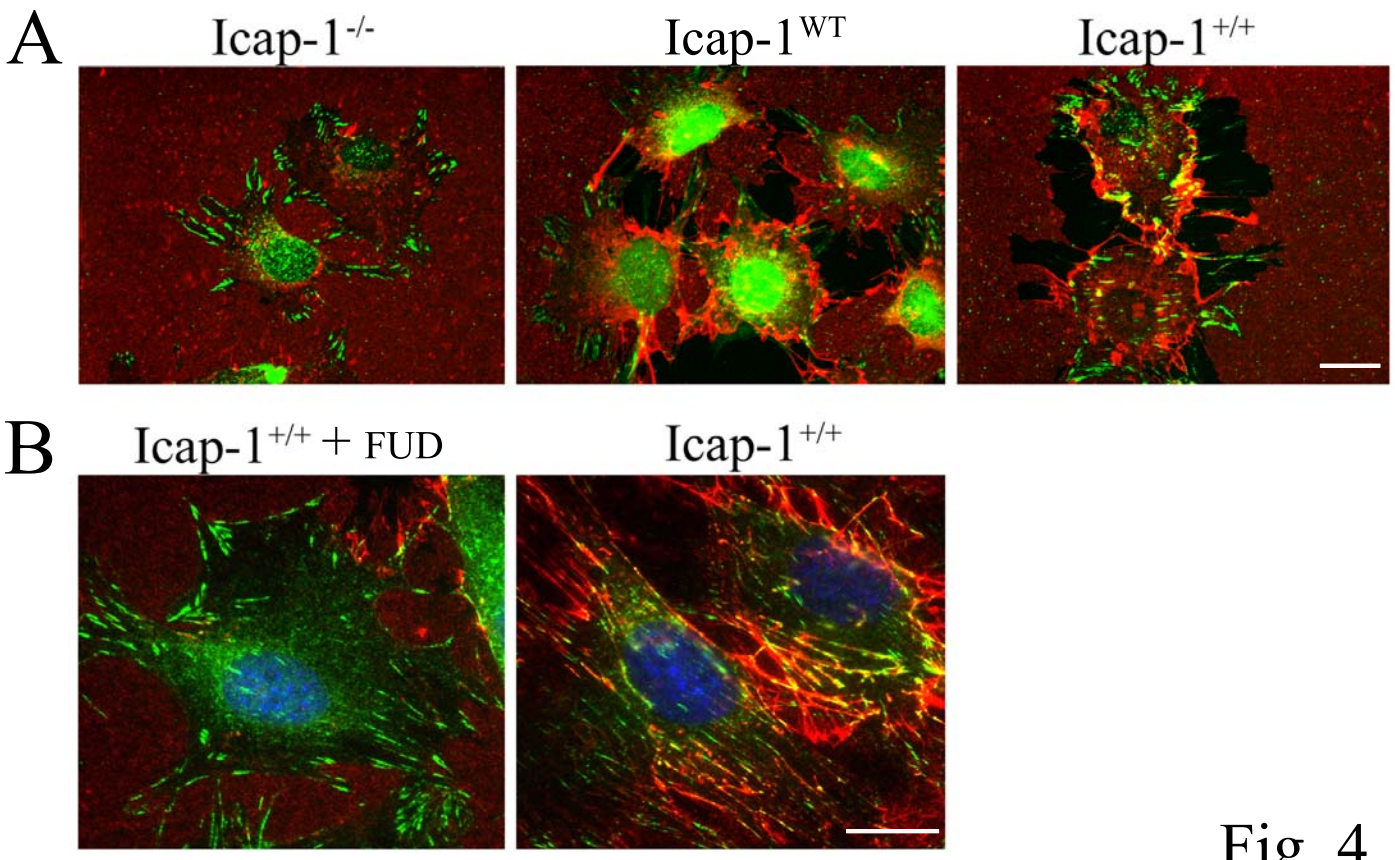
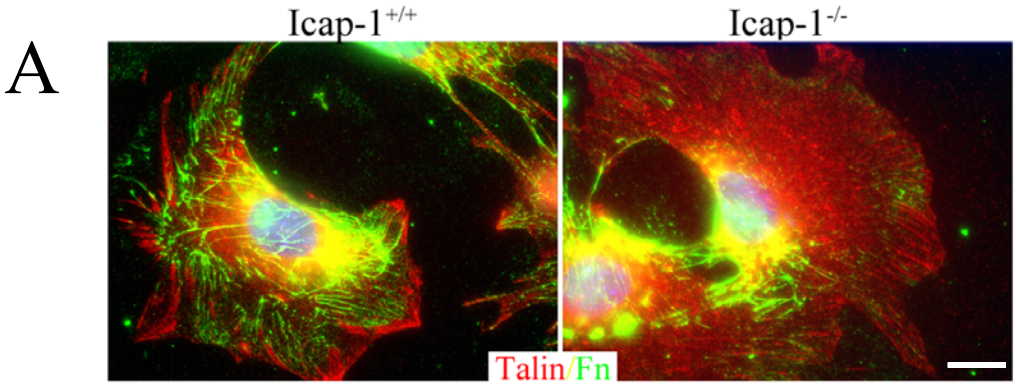
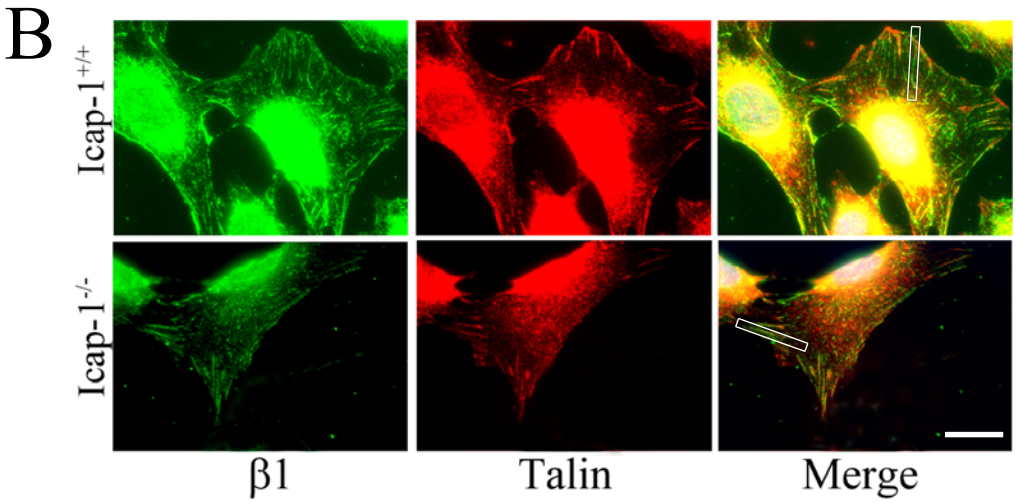


Fig. 4


A
Icap-1+/+
Icap-1-/-
Talin/Fn


B
Icap-1+/+
Icap-1-/-
β1
Talin
Merge

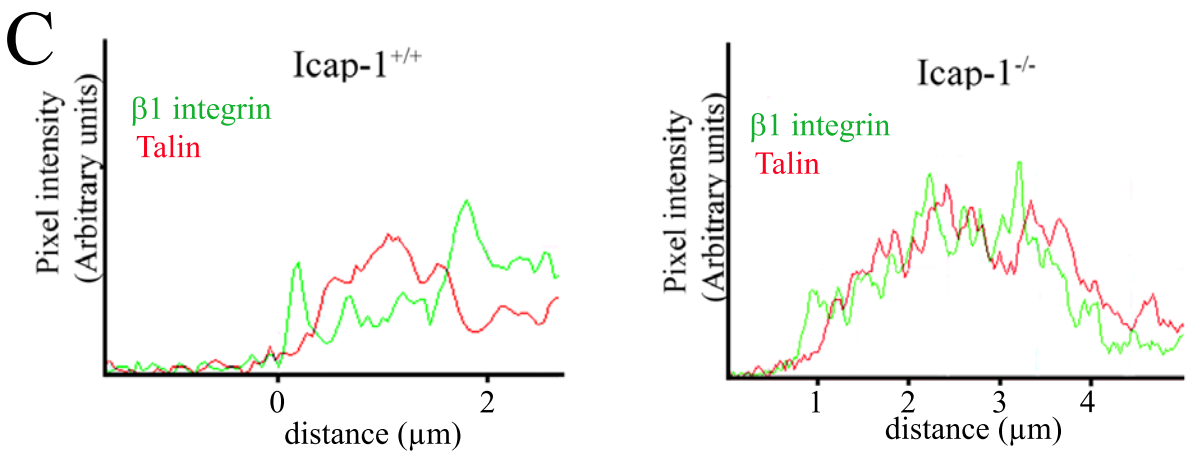

C
Icap-1+/+
β1 integrin
Talin
Pixel intensity (Arbitrary units)
0
2
distance (μm)
Icap-1-/-
β1 integrin
Talin
Pixel intensity (Arbitrary units)
1
2
3
4
distance (μm)

Fig. 5

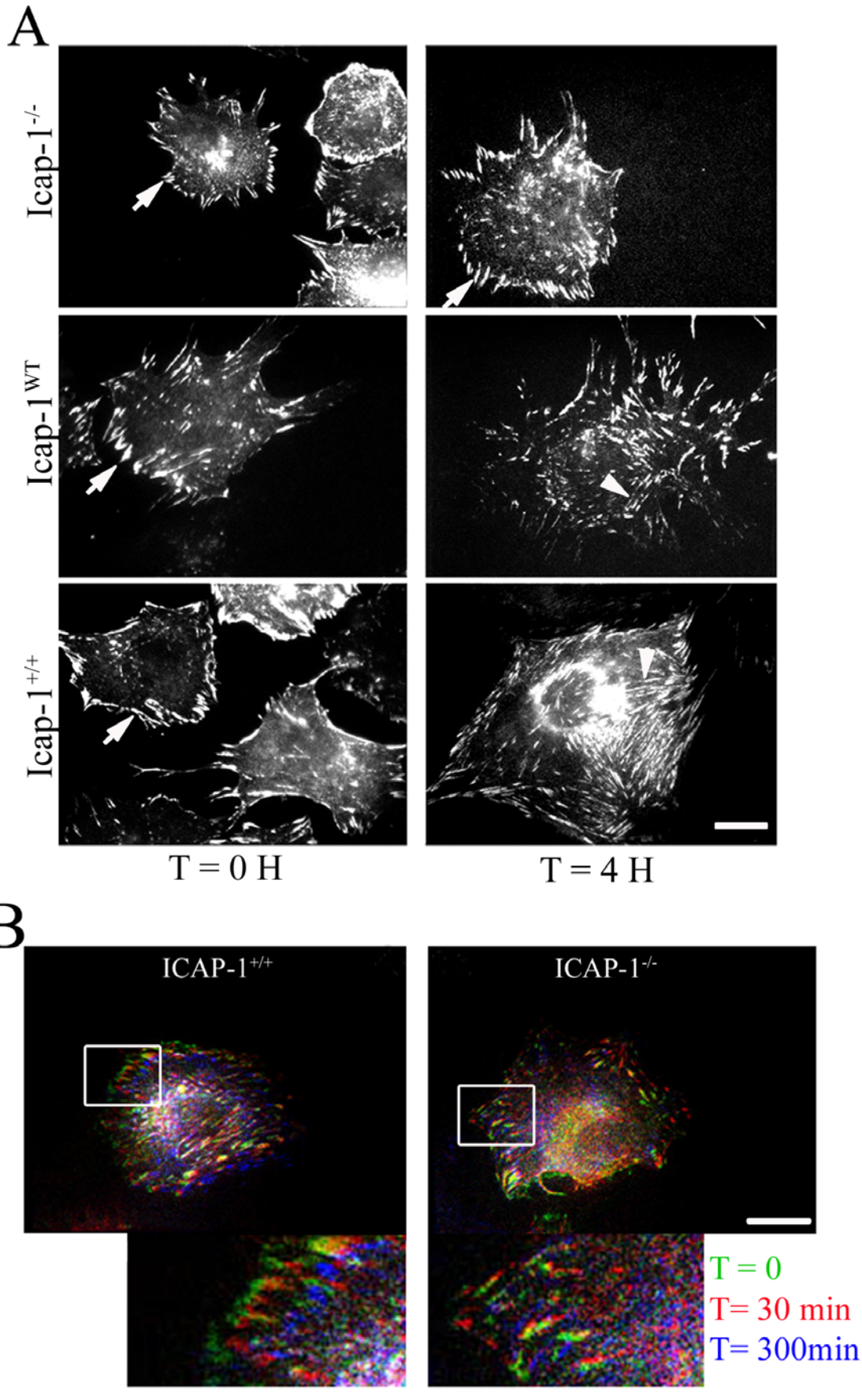

A
Icap-1-/-
Icap-1WT
Icap-1+/+
T = 0 H
T = 4 H
B
ICAP-1+/+
ICAP-1-/-
T = 0
T= 30 min
T= 300min

Fig. 6

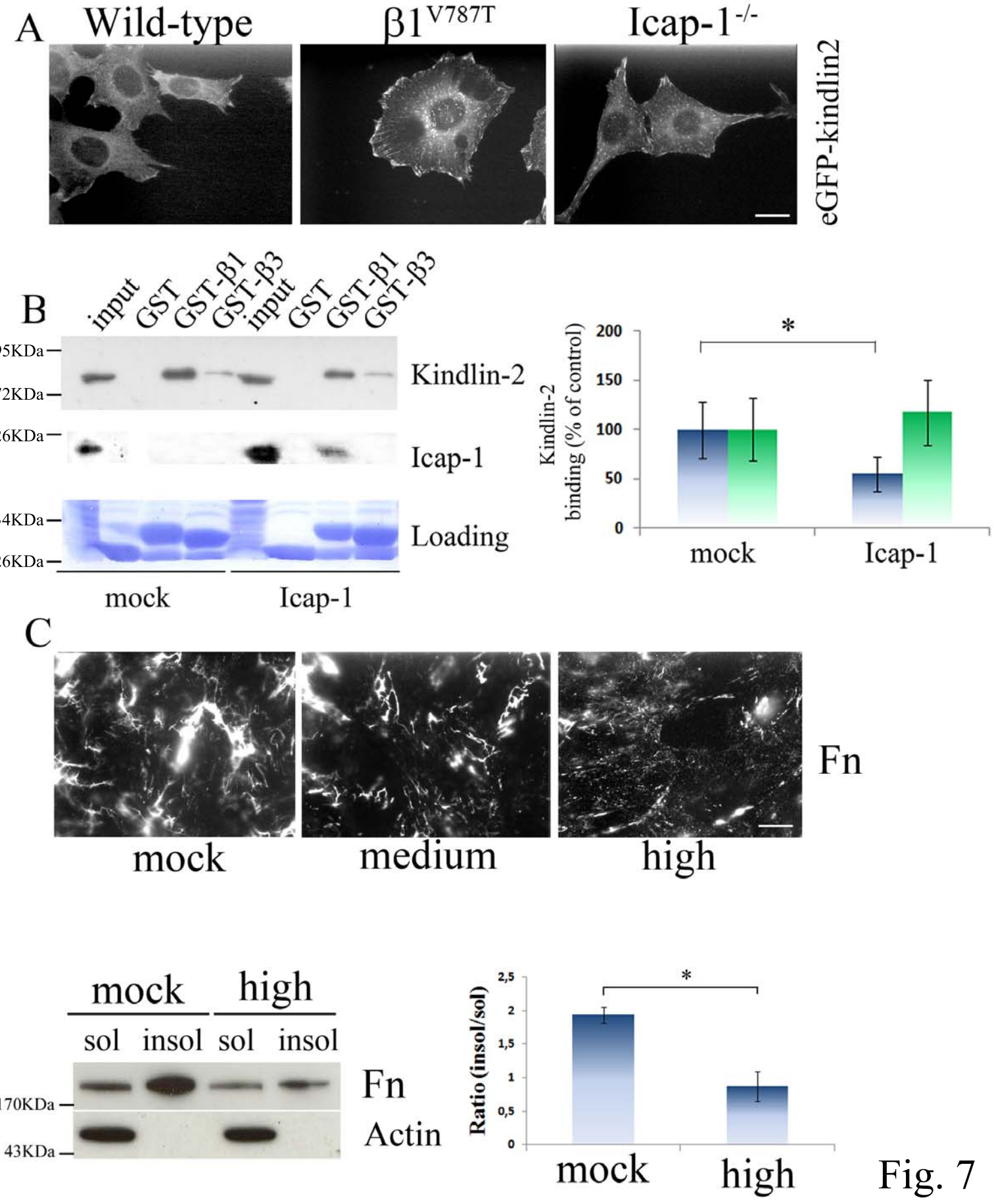

A
Wild-type
β1V787T
Icap-1-/-
eGFP-kindlin2
B
input
GST
GST-β1
GST-β3
input
GST
GST-β1
GST-β3
95KDa
72KDa
26KDa
34KDa
26KDa
Kindlin-2
Icap-1
Loading
mock
Icap-1
Kindlin-2 binding (% of control)
200
150
100
50
0
*
mock
Icap-1
C
Fn
mock
medium
high
mock
high
sol
insol
sol
insol
170KDa
43KDa
Fn
Actin
Ratio (insol/sol)
2,5
2
1,5
1
0,5
0
*
mock
high

Fig. 7

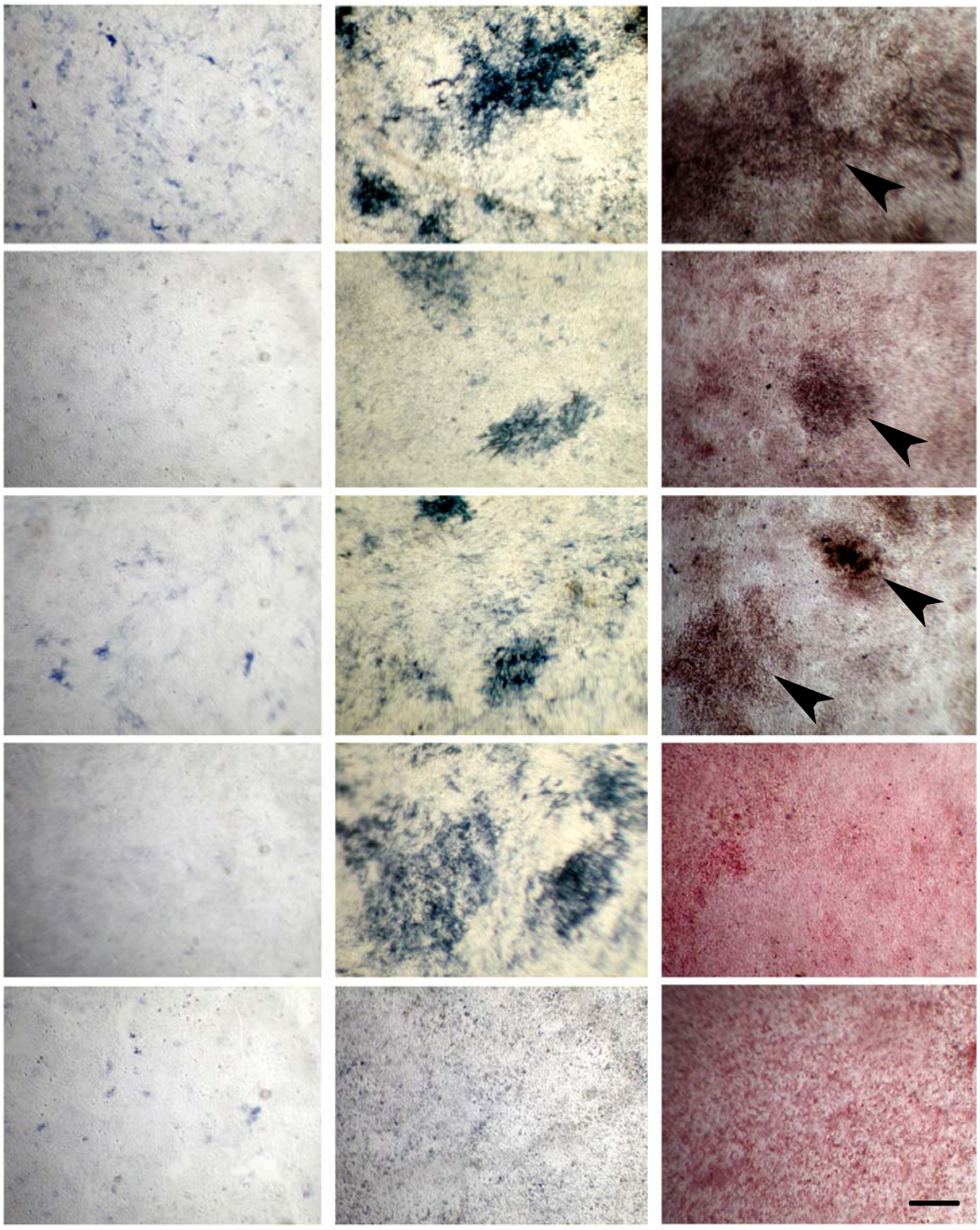


Fig. 8

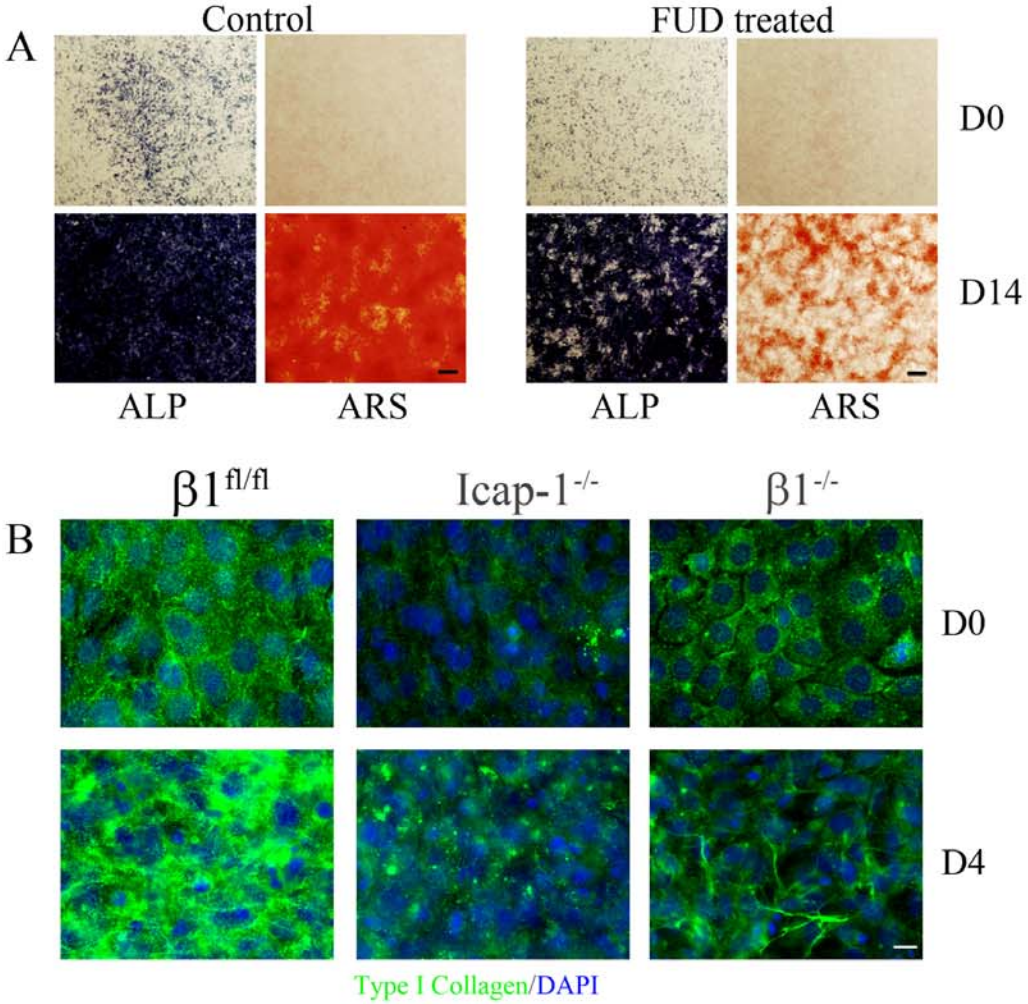
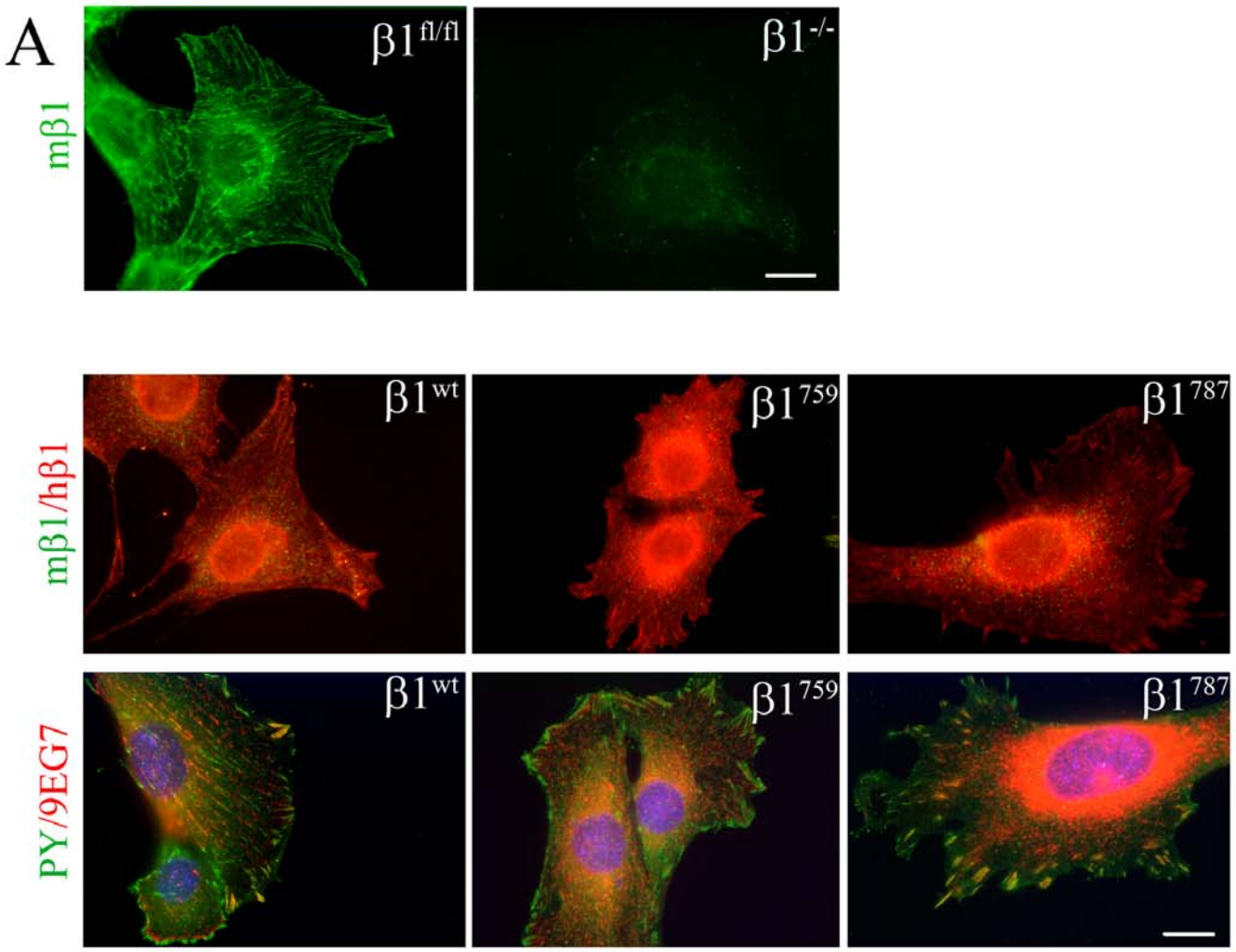

A
Control
FUD treated
D0
D14
ALP
ARS
ALP
ARS
B
β1fl/fl
Icap-1-/-
β1-/-
D0
D4
Type I Collagen/DAPI
C
ARS
Icap–1-/-, D0
Icap–1-/-, D21
β1-/-, D21
β1fl/fl, D21
D
Kindlin-2
mock
high
ALP, D3
ARS, D15

Fig. 9


A
mβ1
β1fl/fl
β1-/-
mβ1/hβ1
β1wt
β1759
β1787
PY/9EG7
β1wt
β1759
β1787

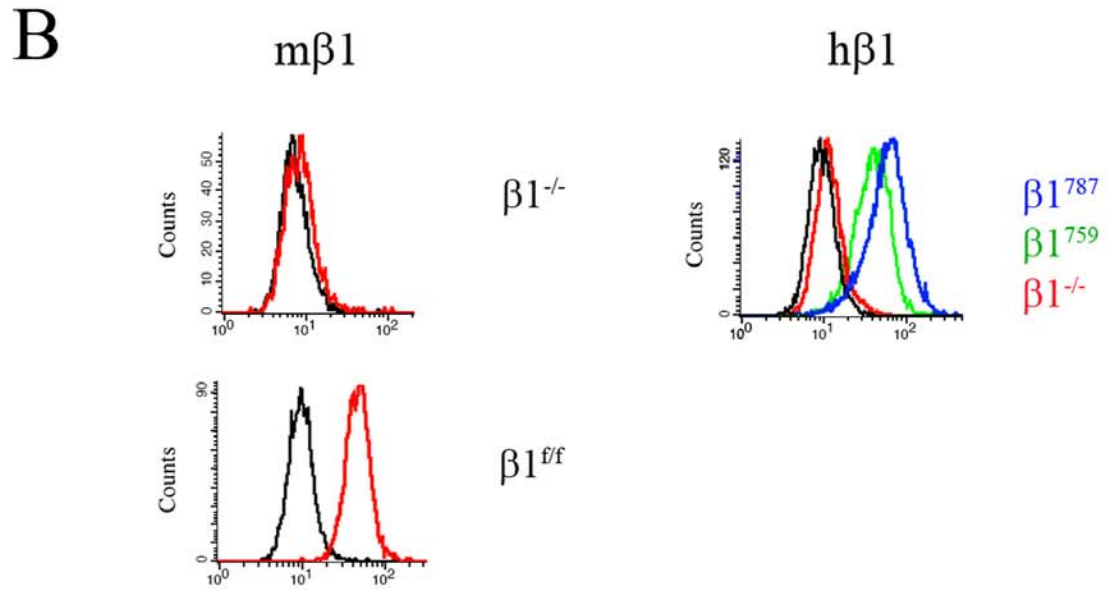

B
mβ1
hβ1
Counts
β1-/-
β1f/f
Counts
β1787
β1759
β1-/-

Fig. S1

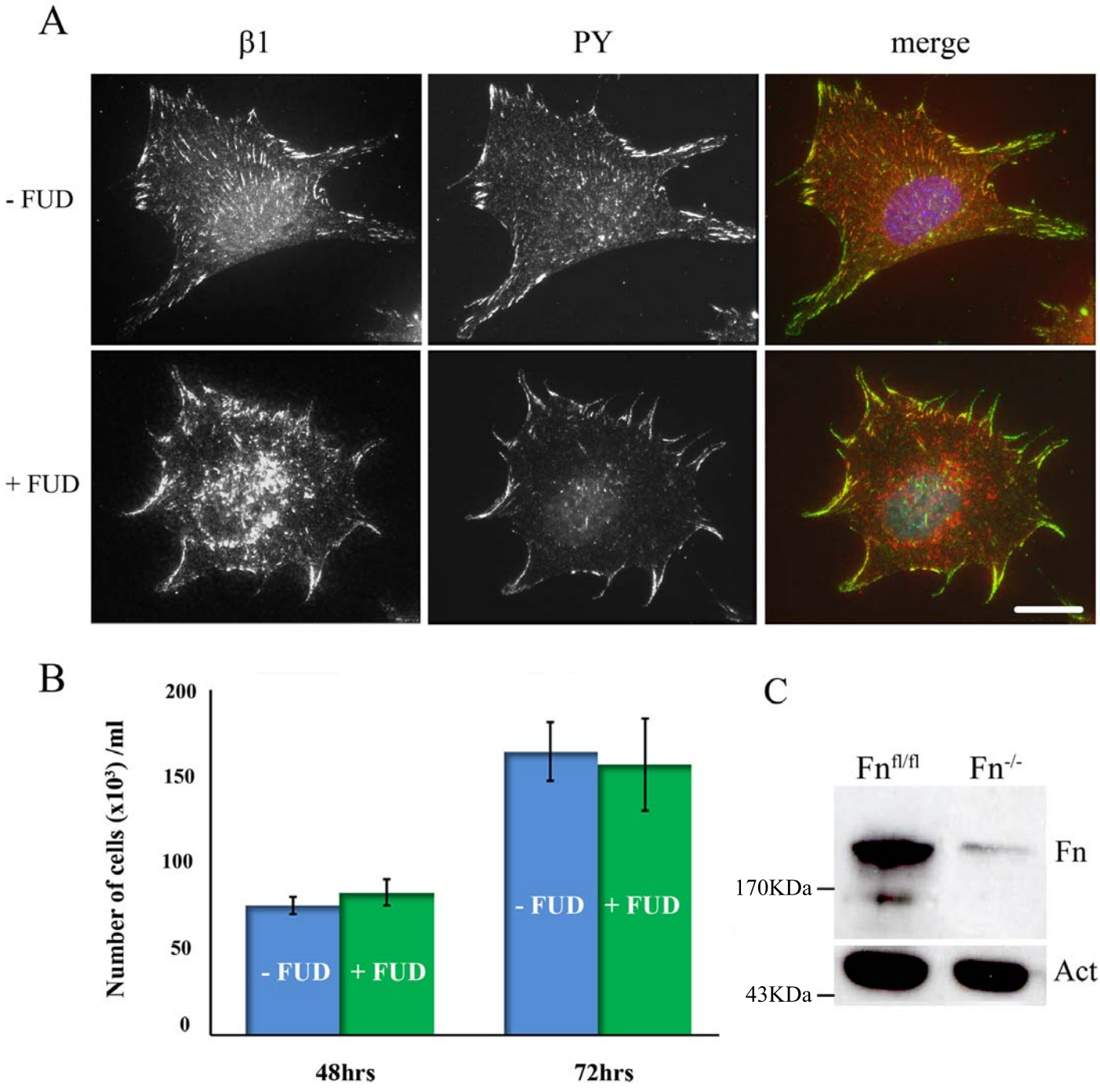

A
β1
PY
merge
- FUD
+ FUD
B
Number of cells (x10³) /ml
200
150
100
50
0
- FUD
+ FUD
- FUD
+ FUD
48hrs
72hrs
C
Fn^fl/fl
Fn^-/-
170KDa
Fn
43KDa
Act

Fig. S2

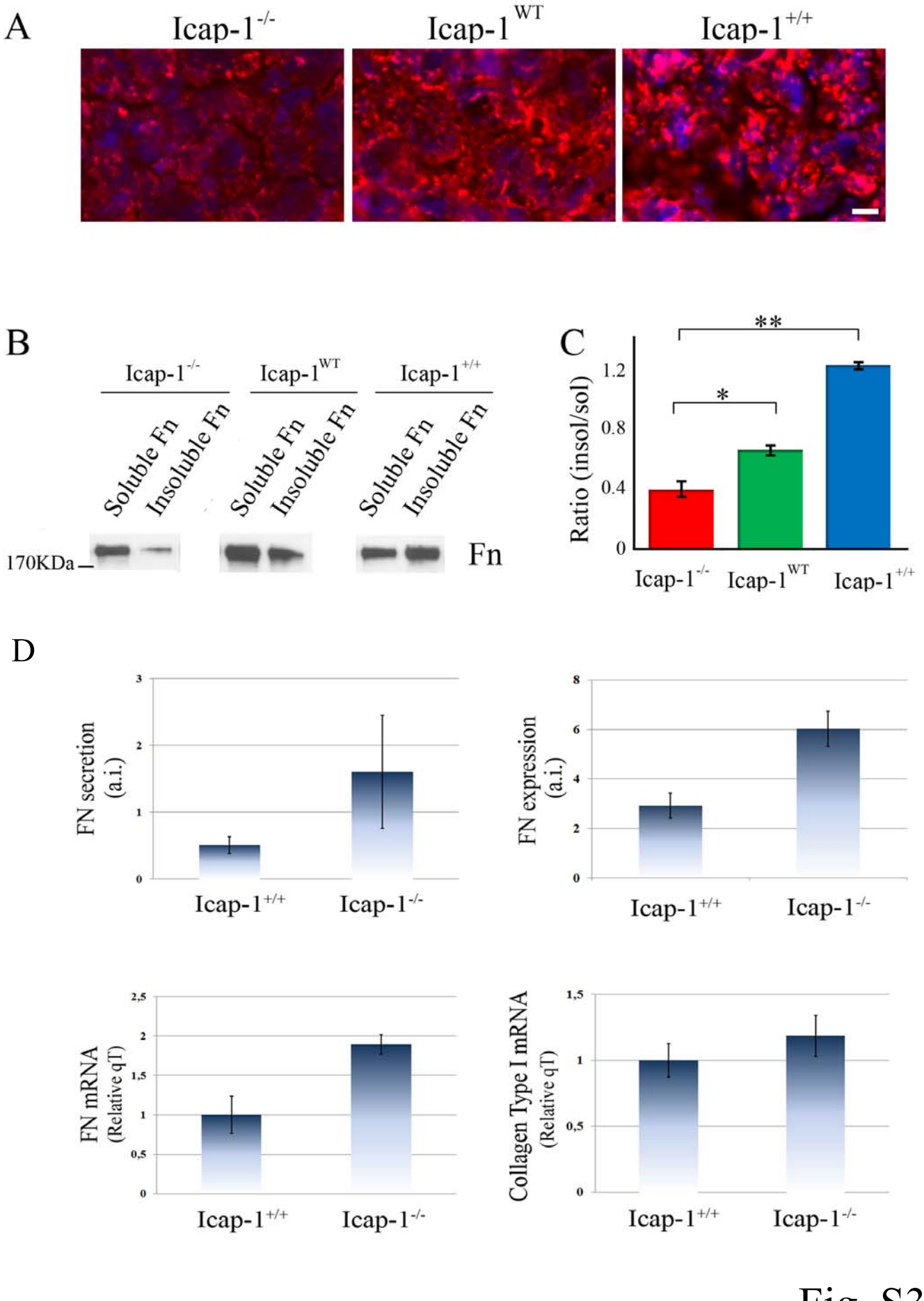

A
Icap-1-/-
Icap-1WT
Icap-1+/+
B
Icap-1-/-
Icap-1WT
Icap-1+/+
Soluble Fn
Insoluble Fn
Soluble Fn
Insoluble Fn
Soluble Fn
Insoluble Fn
170KDa
Fn
C
**
*
Ratio (insol/sol)
1.2
0.8
0.4
0
Icap-1-/-
Icap-1WT
Icap-1+/+
D
FN secretion (a.i.)
3
2
1
0
Icap-1+/+
Icap-1-/-
FN expression (a.i.)
8
6
4
2
0
Icap-1+/+
Icap-1-/-
FN mRNA (Relative qT)
2,5
2
1,5
1
0,5
0
Icap-1+/+
Icap-1-/-
Collagen Type I mRNA (Relative qT)
1,5
1
0,5
0
Icap-1+/+
Icap-1-/-

Fig. S3

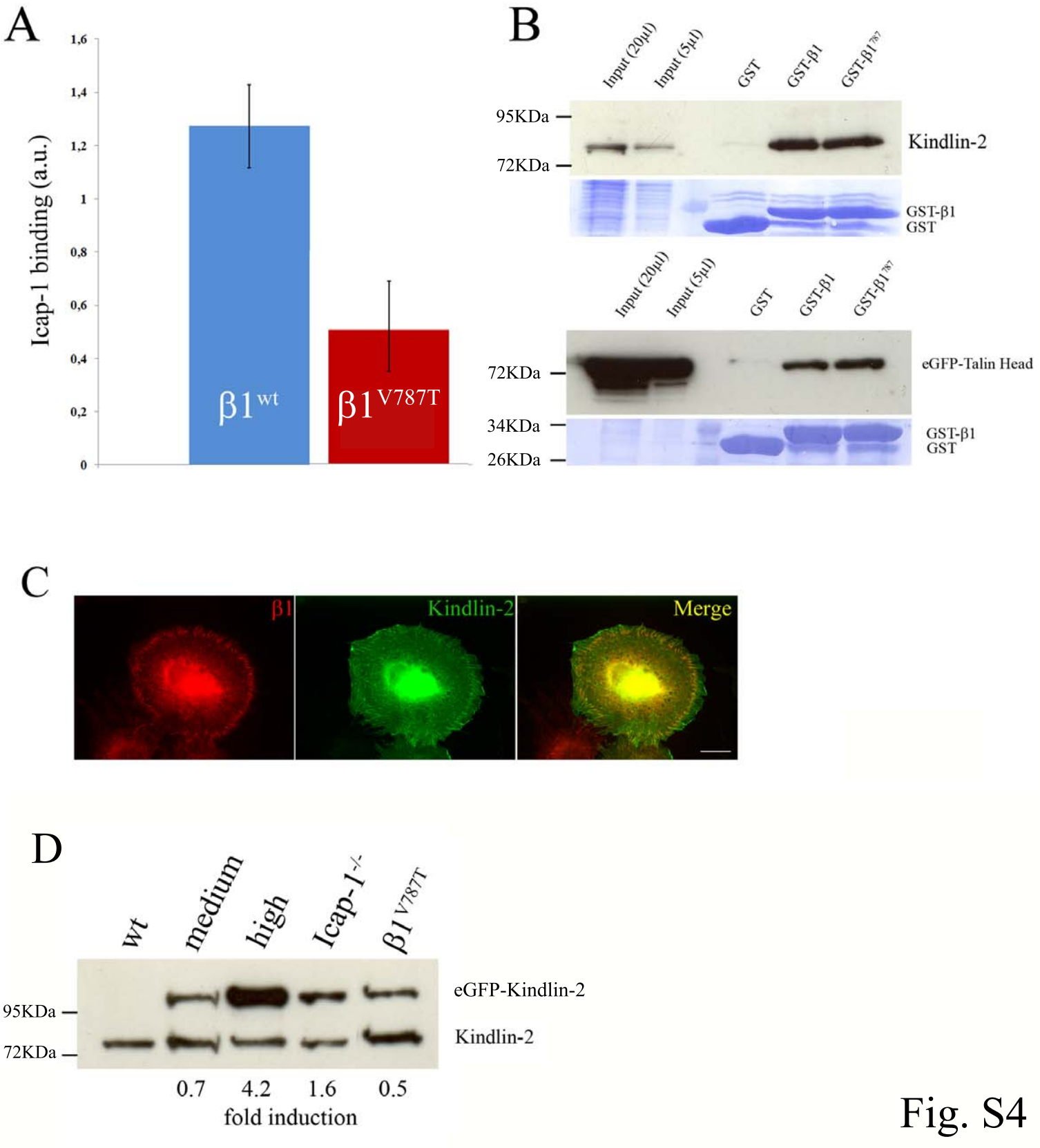

A
Icap-1 binding (a.u.)
1,6
1,4
1,2
1
0,8
0,6
0,4
0,2
0
β1wt
β1V787T
B
Input (20µl)
Input (5µl)
GST
GST-β1
GST-β1787
95KDa
72KDa
Kindlin-2
GST-β1
GST
Input (20µl)
Input (5µl)
GST
GST-β1
GST-β1787
72KDa
eGFP-Talin Head
34KDa
26KDa
GST-β1
GST
C
β1
Kindlin-2
Merge
D
wt
medium
high
Icap-1-/-
β1V787T
95KDa
72KDa
eGFP-Kindlin-2
Kindlin-2
0.7
4.2
1.6
0.5
fold induction

Fig. S4

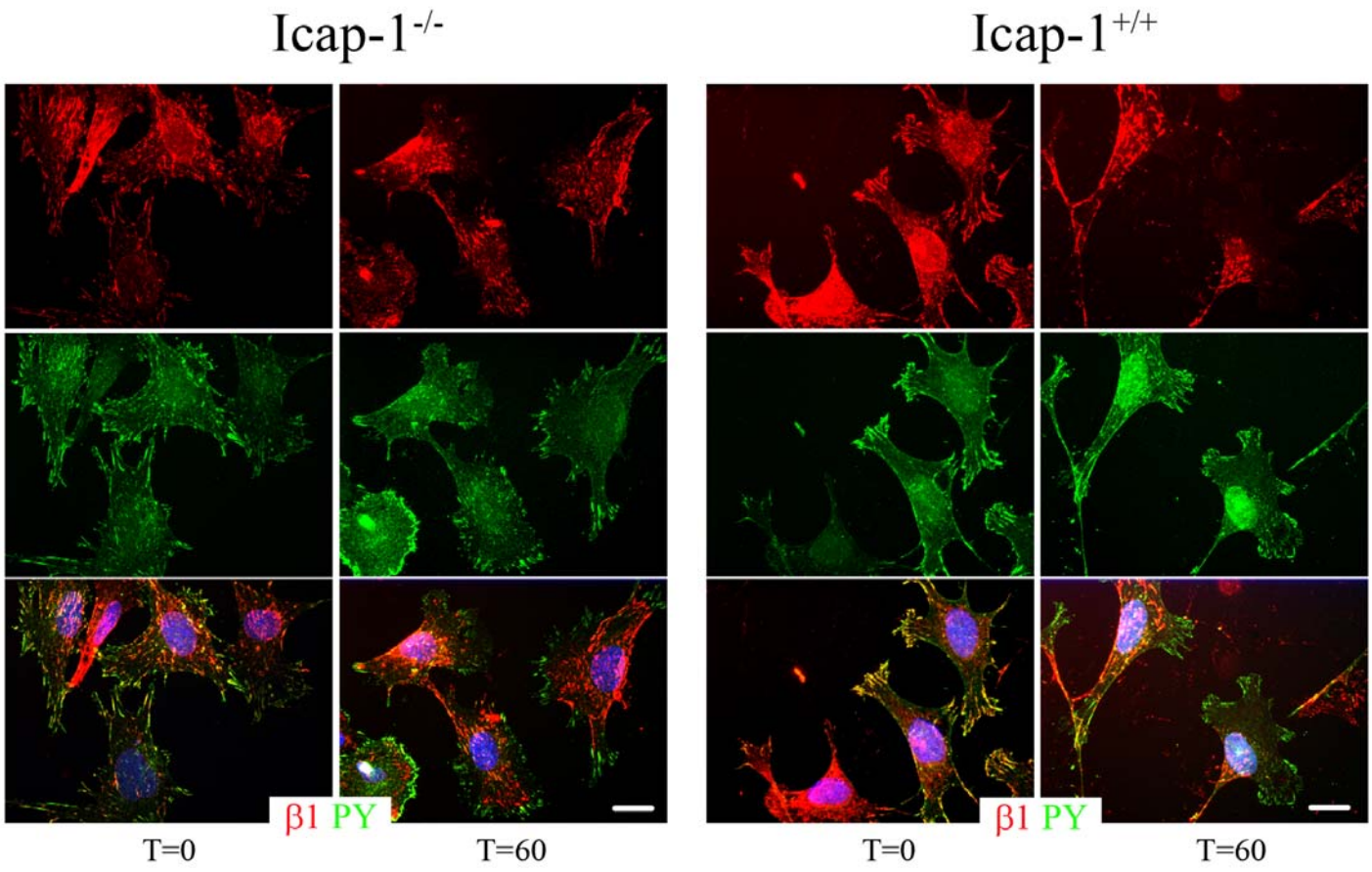


Fig. S5